UNIVERSITÀ DEGLI STUDI DI PADOVA

dSEA

Giovanni Pellegrino
Aarhus University

Efrem Castelnuovo
University of Melbourne
University of Padova

Giovanni Caggiano
Monash University
University of Padova

UNCERTAINTY AND MONETARY POLICY DURING EXTREME EVENTS

August 2020

Marco Fanno Working Papers – 262

Uncertainty and Monetary Policy During Extreme Events*

Giovanni Pellegrino
Aarhus University

Efrem Castelnuovo
University of Padova
University of Melbourne

Giovanni Caggiano
Monash University
University of Padova

August 2020

Abstract

How damaging are uncertainty shocks during extreme events such as the great recession and the Covid-19 outbreak? Can monetary policy limit output losses in such situations? We use a nonlinear VAR framework to document the large response of real activity to a financial uncertainty shock during the great recession. We replicate this evidence with an estimated DSGE framework featuring a concept of uncertainty comparable to that in our VAR. We employ the DSGE model to quantify the impact on real activity of an uncertainty shock under different Taylor rules estimated with normal times vs. great recession data (the latter associated with a stronger response to output). We find that the uncertainty shock-induced output loss experienced during the 2007-09 recession could have been twice as large if policymakers had not responded aggressively to the abrupt drop in output in 2008Q3. Finally, we use our estimated DSGE framework to simulate different paths of uncertainty associated to different hypothesis on the evolution of the coronavirus pandemic. We find that: i) Covid-19-induced uncertainty could lead to an output loss twice as large as that of the great recession; ii) aggressive monetary policy moves could reduce such loss by about 50%.

Keywords: Uncertainty shock, nonlinear IVAR, nonlinear DSGE framework, minimum-distance estimation, great recession, Covid-19.

JEL codes: C22, E32, E52.

* First version: September 2017. We thank Martin M. Andreasen, Susanto Basu, Chris Edmond, Jesús Fernández-Villaverde, Georgios Georgiadis, Pedro Gomis-Porqueras, Pablo Guerron-Quintana, Alejandro Justiniano, Greg Kaplan, Anastasios Karantounias, Fabio Milani, Johannes Pfeifer, Bruce Preston, Eric Swanson, Timo Teräsvirta, Stephen Terry, Trung Duc Tran, Thijs van Rens, and participants at several events for their useful comments. Financial support by the ARC via the Discovery Grants DP160102281 and DP160102654 is gratefully acknowledged. Corresponding author: Efrem Castelnuovo, efrem.castelnuovo@gmail.com.

1 Introduction

"An assumption of linearity may be adequate for estimating average relationships, but few expect that an economy will respond linearly to every aberration." (Greenspan, August 29, 2003)

Financial uncertainty shocks have been identified as one of the drivers of the US business cycle (Bloom (2009), Leduc and Liu (2016), Basu and Bundick (2017), Ludvigson, Ma, and Ng (2019)). Notably, the two highest realizations of the VIX (a popular proxy of financial uncertainty) materialized in correspondence with two of the largest drops in real activity occurred in the last two centuries, i.e., the great recession and the Covid-19 recession.[1] Such dramatic drops in real activity called for immediate and massive interventions by the Federal Reserve to sustain the business cycle. The synchronous occurrence of record large jumps in financial uncertainty, recessions of the magnitude of the 2007-09 one and the one began in 2020, and unprecedented monetary policy interventions begs two connected questions. First, are financial uncertainty shocks relevant contributors to US recessions during extreme events? Second, were monetary policy interventions effective?

This paper addresses these questions by proceeding in three steps. First, we document the response of real activity and monetary policy during the great recession with a nonlinear VAR estimated with post-WWII US data. We identify exogenous variations in uncertainty via the imposition of narrative sign restrictions, an approach recently put forth by Ludvigson, Ma, and Ng (2019) and Antolín-Díaz and Rubio-Ramírez (2019). In particular, we follow Ludvigson, Ma, and Ng (2019) and exploit events in the post-WWII US history characterized by bursts in financial uncertainty that are likely to be informative on the realizations of financial uncertainty shocks. This identification strategy enables us to avoid imposing questionable zero restrictions on the uncertainty-business cycle contemporaneous relationship. We find that nonlinearities are present, statistically relevant, and quantitatively important. In particular, with respect to "normal times", we document a peak response of output 50% larger during the great recession (conditional on a same-size shock), and a peak monetary policy response twice as large (a cut of the federal funds rate of about 100 basis points in normal times vs. 200 basis points during the great recession).

The second step of our analysis estimates a version of the Basu and Bundick (2017)

[1] The VIX reached its historical record level of 82.69 on March 16, 2020. The second highest value ever recorded by the VIX is 80.06, which occurred on October 27, 2008.

model to match our nonlinear VAR stylized facts. We estimate it using the Bayesian minimum-distance direct inference approach developed by Christiano, Trabandt, and Walentin (2010), where we treat as "data" the impulse responses produced with our nonlinear VAR. The presence in the DSGE framework of a theoretical concept of financial uncertainty in line with the proxy we use in our empirical analysis makes Basu and Bundick's model particularly suited to our purposes, because it enables us to match the dynamics of financial uncertainty in the data with its theoretical counterpart. This part of the analysis shows two things. First, the estimated DSGE framework goes a long way in replicating our empirical facts, therefore providing us with an empirically credible microfounded framework to perform factual and counterfactual analysis. Second, the monetary policy response engineered by the Federal Reserve during the great recession (as interpreted by our estimated framework) successfully limited the output cost associated with the spike in financial uncertainty. A comparison between the output loss conditional on the estimated Taylor rule for the great recession, and that conditional on a Taylor rule estimated with impulse responses produced with a linear VAR (which captures systematic monetary policy in normal times), reveals that the stronger response to output growth fluctuations during the great recession possibly halved the uncertainty shock-induced output loss, and shortened the duration of the recession. These exercises are based on state-dependent estimates of our third-order approximated DSGE framework (in normal times vs. during extreme events). To our knowledge, this regime-dependent estimation of a third-order approximated DSGE model is a novel contribution to the literature *per se*.

Finally, we use the model estimated on the great recession data as a laboratory to conduct a scenario analysis on the impact of the Covid-19-induced jump in financial uncertainty occurred in March 2020.[2] In particular, conditional on the formal representation of the economy provided by the Basu and Bundick's (2017) model, we hypothesize three profiles of financial uncertainty, all characterized by a common unanticipated uncertainty shock in March 2020, but different as far as the weight and size of an anticipated uncertainty shock in Fall 2020 are concerned.[3] This latter element

[2]Given that the Covid-19 recession is still unfolding, we have not enough business cycle data to estimate a "Covid-19 version" of our DSGE framework. The use of the model estimated for the great recession to conduct an investigation on the business cycle effects of the Covid-19 pandemic is justified by the comparable jumps in uncertainty at the beginning of the great and Covid-19 recessions, the similarly aggressive policy responses to stabilize output, and (lockdown apart) a similar economic structure in place (chiefly, a similarly high degree of risk aversion in the two extreme events). Section 5 offers further discussions on these assumptions.

[3]This though experiment addresses the question: "What is the contribution of different profiles

is meant to capture agents' expectations over a second wave of coronavirus infections about a semester after the first one, and their implications for the drop in real activity at the end of 2020Q1 and the following quarters. In our worst case scenario, where economic agents expect a second wave of the pandemic to hit in the third quarter of 2020 with larger magnitude than the first, our simulations point to a recession twice as deep as that experienced in 2007-2009, followed by a much slower recovery.[4] Again, we find that an aggressive response to the drop in output growth (which we assume to be similar, in a Taylor rule sense, to the one engineered during the great recession) could substantially dampen the output loss that could otherwise arise because of the Covid-19 uncertainty shock.

Our results offer support to prompt and aggressive policy interventions as those implemented by the Federal Reserve during the great recession and right after the coronavirus pandemic hit the United States in March 2020.[5] From a modeling standpoint, our empirical analysis represents a warning against the use of models estimated in normal times to assess policy interventions engineered during extreme events. In fact, our state-dependent estimation approach unveils regime-dependence of some of the structural parameters of the DSGE framework we work with. The great recession is associated to a stronger systematic monetary policy response to output growth, a higher degree of risk aversion, and higher investment adjustment costs as crucial ingredients to replicate the response of real activity to an uncertainty shock. Hence, paraphrasing Greenspan's quote above, the response of the US economy to the uncertainty shock that materialized during the great recession was indeed an aberration.

The paper develops as follows. Section 2 discusses the related literature. Section 3 presents our non-linear VAR model, the identification strategy we use, and the empirical results. Section 4 describes the DSGE model and the estimation approach; it presents the state-dependent estimation results; it investigates the drivers of the change in the

of financial uncertainty in place from March 2020 onward in an economy which is not characterized by any lockdown, negative labor supply shock, self-isolation behavior, social distancing, and so on?" Most likely, adding any of these elements would increase the magnitude of the real effects of financial uncertainty. Hence, we see our analysis as underestimating the contribution of financial uncertainty shocks on real activity during the Covid-19 pandemic.

[4] To be clear, the emphasis of this exercise is on agents' expectations formulated in March 2020 on the future evolution of the pandemic. The calibration of the most extreme (pessimistic) scenario is inspired by the first two waves of the 1920 Spanish flue. To our knowledge, Barro, Ursúa, and Weng (2020) were the first ones to draw a parallel between the 1920 Spanish Flu and the 2020 Coronavirus pandemic, and to study the economic implications of these two events.

[5] The model we work with in this paper does not explicitly feature unconventional policy interventions (namely, quantitative easing). Following Sims and Wu (2020), we interpret a negative interest rate in presence of the zero lower bound as a close substitute for unconventional policies.

transmission mechanism; and it quantifies the role of monetary policy in mitigating the contractionary impact of uncertainty shock during the great recession. Section 5 uses variants of the baseline DSGE model to simulate different scenarios on the impact of the Covid-19-induced uncertainty shock, and examines the role of monetary policy in tackling the recessionary effects of pandemic-related jumps in uncertainty. Section 6 concludes.

2 Related literature

Our focus on financial uncertainty is due to the recent paper by Ludvigson, Ma, and Ng (2019), who find that shocks to expected financial market volatility are relevant drivers of the US business cycle. We borrow their identification strategy to isolate exogenous changes in financial uncertainty and quantify their effects on the business cycle. There are three fundamental differences between our paper and theirs. First, we use a nonlinear framework to distinguish the macroeconomic responses to uncertainty shocks in normal times and during the great recession. Second, we identify financial uncertainty shocks by appealing to a larger set of restrictions with respect to theirs. Third, we interpret our responses by taking Basu and Bundick's (2017) microfounded DSGE model to the data, and by using it to assess the role played by systematic monetary policy to contrast the negative real activity effects due to the great recession and Covid-19 uncertainty shocks. Differently, Ludvigson, Ma, and Ng (2019) focus on the identification of the real effects of uncertainty shocks in a VAR-only context.

Methodologically, we use a nonlinear Interacted VAR (IVAR) model to establish novel facts regarding the different impact of financial uncertainty shocks on a battery of real activity indicators. In computing our impulse responses, we follow Pellegrino (2017,2018) and Caggiano, Castelnuovo, and Pellegrino (2017) and allow both uncertainty and real activity - i.e., the elements composing the interaction terms in our nonlinear VAR - to endogenously evolve after an uncertainty shock. We do so to minimize the bias in our estimated responses that could otherwise emerge if uncertainty were not allowed to be endogenous and, above all, the business cycle were not allowed to react to shocks in uncertainty. Our IVAR-related findings, which point to more severe consequences of uncertainty shocks for output, investment, consumption, and hours during the great recession compared to normal times, echo those by Caggiano, Castelnuovo, and Groshenny (2014) on unemployment, and those obtained with indicators correlated with the business cycle like financial stress (Alessandri and Mumtaz (2019)).

Differently from these contributions, which analyze a generic recession, our focus is on extreme events such as the great recession and the Covid-19 outbreak.

As anticipated above, we estimate a version of Basu and Bundick's (2017) framework with the impulse-response matching approach popularized by Christiano, Trabandt, and Walentin (2010). Given that we do this in a state-dependent fashion (i.e., we estimate our model separately with impulse responses related to normal times vs. the great recession), we are able to unveil instabilities in the systematic monetary policy parameters which we then exploit in our simulation exercises. With respect to Basu and Bundick (2017), our stylized facts are obtained with a nonlinear VAR framework, which we use to show that the response of real activity to an uncertainty shock is economically and significantly larger during the great recession than in normal times. The state-dependent estimation of their framework points to relevant instabilities in a few structural parameters - in particular, our evidence points to a higher degree of risk aversion, higher investment adjustment costs, and a stronger monetary policy response to output growth during the great recession.[6] Finally, we employ the estimated DSGE framework to shed light on the role of systematic monetary policy in the aftermath of the Covid-19 uncertainty shock.

Methodologically, the closest approach to ours is probably the one by Ruge-Murcia (2014), who estimates a small-scale third-order approximated DSGE model with an impulse-response matching procedure based on a class of nonlinear VARs as auxiliary models for the purpose of indirect inference via a classical minimum distance estimator. In doing so, he imposes the perturbation solution of the nonlinear DSGE model on the nonlinear VAR framework to approximate as closely as possible the DSGE-related policy functions. His approach, which is extremely neat, becomes unfortunately difficult to implement when one works with models with several states. Our novel estimation strategy easily accommodates large state spaces.

[6] While writing this paper, we found out a related contribution Bretscher, Hsu, and Tamoni (2018). They also find that risk aversion acts as a magnifier of the real effects of uncertainty shocks. Our analysis differs in many respects. First, we find that changes in investment adjustment costs and the systematic monetary policy response to output growth are also important to describe the response of real activity to an uncertainty shock during the great recession. Second, we establish stylized facts with a nonlinear VAR where uncertainty shocks are identified using a state-of-the-art narrative sign restrictions approach. Third, we take our DSGE framework to the data by matching the nonlinear impulse responses of our VAR, therefore allowing for a state-dependent estimation of the micro-founded framework we work with. Fourth, we quantify the role played by an aggressive policy rule (in terms of output stabilization) during extreme events such as the great recession and Covid-19 (their paper is concerned with the former, and does not cover the latter). Finally, when studying the Covid-19 pandemic, we engineer simulations combining unexpected and anticipate uncertainty shocks, while they only study the former type of shock.

Finally, our work is related to several recent contributions that have attempted at quantifying the impact on real activity of the Covid-19-induced uncertainty shock. Baker, Bloom, Davis, and Terry (2020) feed the estimated model of disaster risk by Baker, Bloom, and Terry (2020) with first and second moment financial shocks calibrated to match the fall observed in the US stock market and the rise in implied volatility between February and March 2020. They find that the uncertainty shock due to Covid-19 reduces output by about 11% over a one year horizon. Ludvigson, Ma, and Ng (2020) construct a series of costly disaster for the US, which they then use in VAR to simulate the effects of a multi-period shock generated by the pandemic. They find that, in a conservative case of a shock lasting three months, industrial production is expected to fall by 12.75% in 2020. Pellegrino, Ravenna, and Züllig (2020) use a nonlinear VAR to account for the role played by agents' expectations. They quantify the impact of an uncertainty shock calibrated to match the jump in financial volatility observed in March 2020 conditional on very negative expectations about the future economic outlook, and find that industrial production will experience a drop in between 15% and 19% by the end of 2020. With respect to all these contributions, we: i) show that uncertainty shocks have particularly powerful business cycle effects during extreme events (the great recession being the one we target with our VAR analysis); ii) show that an estimated DSGE framework can successfully replicate the dynamics in normal times and during the great recessions triggered by an uncertainty shock; iii) conduct simulations with such a framework to compare the output costs due to uncertainty shocks during the great recession and to the Covid-19 outbreak, and associate the latter event with different (alternative) scenarios on the evolution of the Covid-19 pandemic, among which we also consider the hypothesis of expectations of a second wave in Fall 2020; iv) document the role played by a switch to a more aggressive monetary policy as far as output stabilization is concerned.

3 The real effects of uncertainty shocks: Empirical evidence

3.1 Nonlinear empirical methodology

Reduced-form nonlinear VAR. We represent the US macroeconomic environment with an IVAR, which augments a standard linear VAR model with interaction terms to determine how the effects of a shock to a variable depend on the level of another

conditioning variable. Following Pellegrino (2017a,b) and Caggiano, Castelnuovo, and Pellegrino (2017), we focus on a parsimonious IVAR to maximize the available degrees of freedom while capturing the nonlinearity of interest.

Our IVAR is the following:

$$\mathbf{Y}_t = \boldsymbol{\alpha} + \sum_{j=1}^{L} \mathbf{A}_j \mathbf{Y}_{t-j} + \left[\sum_{j=1}^{L} \mathbf{c}_j \ln VXO_{t-j} \times \Delta \ln GDP_{t-j} \right] + \boldsymbol{\eta}_t, \quad \boldsymbol{\eta}_t \sim d(0, \boldsymbol{\Omega}) \quad (1)$$

where $\mathbf{Y}_t$ is the $(n \times 1)$ vector of the endogenous variables, $\boldsymbol{\alpha}$ is the $(n \times 1)$ vector of constant terms, $\mathbf{A}_j$ are $(n \times n)$ matrices of coefficients, and $\boldsymbol{\eta}_t$ is the $(n \times 1)$ vector of error terms whose variance-covariance (VCV) matrix is $\boldsymbol{\Omega}$, and $d(\cdot)$ is the distribution of the residuals. The interaction term in brackets makes an otherwise standard VAR a non-linear IVAR model. For each lag j, such interaction term includes a $(n \times 1)$ vector of coefficients $\mathbf{c}_j$, a measure of uncertainty $\ln VXO_t$, and an indicator of the business cycle $\Delta \ln GDP_{t-j} \equiv \ln GDP_{t-j} - \ln GDP_{t-j-1}$, which is the quarter-on-quarter growth rate of real GDP. The interaction term $\ln VXO_{t-j} \times \Delta \ln GDP_{t-j}$ enables us to capture the potentially state-contingent effects of a shock to $\ln VXO_{t-j}$ (i.e., an uncertainty shock) conditional on the state of the business cycle, which is proxied by the growth rate of real GDP.

Alternatives to IVAR frameworks - such as, e.g., regime switching frameworks or smooth transition VARs - are available to capture the nonlinear effects of macroeconomic shocks (for a recent survey, see Teräsvirta (2018)). We prefer to employ the IVAR framework (1) for three reasons. First, it closely resembles the approximated nonlinear policy functions of the DSGE framework we work with.[7] Second, it allows uncertainty shocks to have different effects over time because of the changing business cycle stance, which is key to isolate the impact of uncertainty during a specific recession. Third, it does not feature nuisance parameters, which are often difficult to estimate in nonlinear frameworks.[8]

Data. We model the vector $\mathbf{Y}_t = [\ln VXO, \ln GDP, \ln C, \ln I, \ln H, \ln P, R]'$, where VXO denotes the stock market S&P 100 implied volatility index, GDP per capita GDP, C per capita consumption, I per capita investment, H per capita hours worked,

[7] Nonlinear policy functions feature different, higher order interaction terms. We focus on terms featuring uncertainty and the real GDP growth because of our interest in isolating the impact of uncertainty shocks during the 2008-2009 downturn. Simulations conducted with higher order terms, and reported in our Appendix, deliver even stronger empirical results in favor of such nonlinear effects.

[8] Notice that IVARs featuring interactions terms resemble approximated Smooth Transition VAR frameworks (Teräsvirta, Tjøstheim, and Granger (2010)).

P the price level, and R the policy rate. The variables in this vector are those used by Basu and Bundick (2017) in their linear VAR analysis.[9] We estimate our IVAR model with four lags over the 1962Q3-2017Q4 sample. Given that the VXO is unavailable before 1986, we follow Bloom (2009) and splice it with the within-month volatility of S&P500 daily returns, which has displayed an extremely high correlation with the VXO since 1986. The sample includes the zero lower bound period experienced by the Federal Reserve during the period 2008Q4-2015Q4. We then work with the shadow rate constructed by Wu and Xia (2016) to account for the effects of unconventional policy responses to financial uncertainty shocks.

A standard likelihood-ratio test favors our IVAR specification against the Basu and Bundick's (2017) linear VAR model (which is nested in our IVAR model in case of the overall exclusion of the interaction terms from model (1)). In particular, the LR test suggests a value for the test statistic $\chi_{28} = 61.99$, which allows us to reject the null hypothesis of linearity at any conventional statistical level in favor of the alternative of our I-VAR model (p-value $<< 0.01$).

Identification. We move from the reduced-form IVAR in (1) to the structural one as follows. First, we assume that the system of contemporaneous relationships mapping reduced form residuals $\boldsymbol{\eta}_t$ and structural shocks $\mathbf{e}_t$ can be described as

$$\boldsymbol{\eta}_t = \boldsymbol{B}\mathbf{e}_t, \quad \mathbf{e}_t \sim d(0, \boldsymbol{I_n}) \tag{2}$$

where $\boldsymbol{B}$ is a matrix featuring n^2 elements. Given that the reduced form covariance matrix $\boldsymbol{\Omega}$ features only $n(n+1)/2$ restrictions, further restrictions have to be imposed to identify the effects of the structural shocks $\mathbf{e}_t$ on the endogenous variables $\mathbf{Y}_t$. Without such further restrictions, infinitely many solutions satisfy the covariance restrictions $\boldsymbol{\Omega} = \boldsymbol{BB'}$. We collect these uncountably many solutions into the set $\mathcal{B} = \{\boldsymbol{B} = \boldsymbol{PQ} : \boldsymbol{Q} \in \mathcal{O}_n, diag(\boldsymbol{B}) \geqslant 0, \boldsymbol{\Omega} = \boldsymbol{BB'}\}$, where $\mathcal{O}_n$ is the set of $(n \times n)$ orthonormal matrices (i.e., $\boldsymbol{QQ'} = \boldsymbol{I_n}$), $\boldsymbol{P}$ is the unique lower-triangular Cholesky factor with non-negative diagonal elements, i.e., $\boldsymbol{\Omega} = \boldsymbol{PP'}$.

The set $\mathcal{B}$ is constructed by implementing the algorithm proposed by Rubio-Ramírez, Waggoner, and Zha (2010). First, we initialize the algorithm by setting $\boldsymbol{B} = \boldsymbol{P}$. Then, we rotate $\boldsymbol{B}$ by randomly drawing one million matrices $\boldsymbol{Q}$. Each rotation is performed by drawing a $(n \times n)$ matrix $\boldsymbol{M}$ from a $\mathcal{N}(\mathbf{0}, \boldsymbol{I_n})$ density. Then, $\boldsymbol{Q}$ is taken to be

[9] Basu and Bundick's (2017) VAR also features the presence of money. Adding money implies no changes in our empirical results. The definition and construction of the variables common to our investigations is exactly the same as in Basu and Bundick (2017).

the orthonormal matrix in the QR decomposition of $\boldsymbol{M}$. Given that $\boldsymbol{B} = \boldsymbol{PQ}$ and $\boldsymbol{QQ}' = \boldsymbol{I_n}$, the covariance restrictions $\boldsymbol{\Omega} = \boldsymbol{BB}'$ are satisfied. Let $\mathbf{e}_t(\boldsymbol{B}) = \boldsymbol{B}^{-1}\boldsymbol{\eta}_t$ be the shocks implied by $\boldsymbol{B} \in \mathcal{B}$ for a given $\boldsymbol{\eta}_t$. Then, one million different $\boldsymbol{B}$ imply one million unconstrained $\mathbf{e}_t(\boldsymbol{B}) = \boldsymbol{B}^{-1}\boldsymbol{\eta}_t$, $t = 1, ..., T$.

While the set $\mathcal{B}$ contains infinitely many solutions mathematically coherent with equations (1)-(2), not all these solutions are equally credible from an economic standpoint. Following Ludvigson, Ma, and Ng (2019), we impose shock-based restrictions to select the economically interesting shocks. In particular, we impose restrictions directly on the shocks $\mathbf{e}_t(\boldsymbol{B})$ to work out the set of admissible solutions $\overline{\mathcal{B}}$ that can be considered as economically sensible. We identify uncertainty shocks by working with two types of restrictions, i.e., event constraints and external variable constraints.

Event constraints. Event constraints are justified by large jumps in financial uncertainty which have a clear interpretation from an historical standpoint. Figure 1 plots the financial uncertainty measure used in this study and identifies the events we work with. In our estimation sample, the two largest peaks occur in 1987Q4 (Black Monday in October 1987) and in 2008Q4 (acceleration of the financial crisis after the collapse of Lehman Brothers). For a financial uncertainty shock to be credible, we require it to be larger than the 75th percentile of the empirical distribution of the realizations of financial uncertainty shocks $\mathbf{e}_{FUt}(\boldsymbol{B})$ in 1987Q4 and 2008Q4.[10] Other two peaks we target are the ones in 1979Q4 and 2011Q3, which correspond to the beginning of the Volcker experiment (targeting of non-borrowed reserves) and to the debt-ceiling crisis, respectively. We require the realizations of our identified uncertainty shocks to be larger than the median value of the empirical density of the uncertainty shocks $\mathbf{e}_{FUt}(\boldsymbol{B})$ in these two dates. These four restrictions are those imposed by Ludvigson, Ma, and Ng (2019) for the identification of their financial uncertainty shocks. In an attempt to sharpen our VAR's ability to correctly identify financial uncertainty shocks, we then add further constraints. In particular, we consider all events identified by Bloom (2009) as possibly related to exogenous variations in financial uncertainty.[11] These events include, among others, the assassination of JFK, two OPEC crisis, two Gulf wars, 9/11, the Asian crisis, and the LTCM default. Bloom's (2009) sample ends in June 2008.

[10] This paper focuses on financial uncertainty. Ludvigson, Ma, and Ng (2019) jointly deal with financial and macroeconomic uncertainty, and require either one or the other (or both) to be large during the great recession. Interestingly, they find financial uncertainty shocks to be largely prevailing in correspondence to the spike in uncertainty in late 2008. A related paper that emphasizes the role of financial uncertainty as a driver of the business cycle during the great recession is Angelini, Bacchiocchi, Caggiano, and Fanelli (2019)

[11] Bloom (2009) reports the list of these events in Table A.1, page 676.

When checking peaks in financial uncertainty in more recent times, we identify one in 2016Q1. Several uncertainty-triggering events occurred right before or during this quarter, e.g., the first increase of the federal funds rate which ended the zero lower bound phase after seven years; fears about China's economic fragility; the Central Bank of Japan going negative with the policy rate; and the announcement in February 2016 by British Prime Minister David Cameron of the Brexit referendum in June that year. For all these events (Bloom's plus those related to 2016Q1), we impose that our identified shocks must be larger than the median value of the empirical density of the uncertainty shocks $\mathbf{e}_{FUt}(\boldsymbol{B})$. Table 1 reports all the event constraints we work with.

External variable constraints. We further narrow down the set of models surviving the selection conditional on the event constraints described above by imposing external variable constraints. Again following Ludvigson, Ma, and Ng (2019), we impose two such constraints. We impose that the correlation between $\mathbf{e}_{FUt}(\boldsymbol{B})$ and the aggregate stock market returns (growth rate of the real price of gold) to be below (above) the median of its empirical density. The rationale for these constraints is the negative correlation between financial volatility and stock market returns typically predicted by macro-finance models, and the role of gold as a safe asset investors go to when financial uncertainty is high.[12] These two constraints are also indicated in Table 1.

Generalized impulse responses. The interaction term of our IVAR is treated as an endogenous object. We compute GIRFs à la Koop et al. (1996) to account for both the endogenous response of the growth rate of per capita GDP, i.e., our conditioning variable, to the uncertainty shock and the feedback this reaction can imply on the dynamics of the economy. Theoretically, the GIRF at horizon h of the vector $\mathbf{Y}_t$ to a shock of size δ computed conditional on an initial history $\boldsymbol{\varpi}_{t-1} = \{\mathbf{Y}_{t-1}, ..., \mathbf{Y}_{t-L}\}$ is given by the following difference of conditional expectations:

$$GIRF_{Y,t}(h, \delta_t, \varpi_{t-1}) = E\left[\mathbf{Y}_{t+h} \mid \delta, \varpi_{t-1}\right] - E\left[\mathbf{Y}_{t+h} \mid \varpi_{t-1}\right].$$

In our analysis, we are interested in recovering the response of $\mathbf{Y}_t$ to an uncertainty shock conditional on a specific initial history $\boldsymbol{\varpi}_{t-1} = \{\mathbf{Y}_{t-1}, ..., \mathbf{Y}_{t-4}\}$, where $t-1 = 2008Q3$, the initial history that corresponds to the quarter before the remarkable uncertainty spike in 2008Q4 (see Figure 1). Hence, the IVAR GIRFs $\widehat{\boldsymbol{\psi}^i}$ for the great recession are

[12] As stressed by Ludvigson et al. (2019), the external variables used here are not required to be valid exogenous instruments. Hence, this identification approach is conceptually different with respect to the one used in the proxy-SVAR literature. For a contribution in this latter direction, see Piffer and Podstawski (2018).

computed by iterating forward the system starting from the initial condition ϖ_{2008Q3}. Our Appendix describes the algorithm used to compute the GIRFs. As regards the size of the shock δ, we impose a 4.4 standard deviation shock, which is the median size of the uncertainty shock in $t = 2008Q4$ among all retained shocks series.

3.2 Empirical results

Figure 2 plots the generalized impulse responses computed with our IVAR approach for the great recession and the impulse responses obtained with the nested linear VAR. The figure reports the identified set of impulse responses along with the median target impulse response both for normal times and for the great recession.[13] To better appreciate the quantitative differences between the responses in normal times and those related to the great recession, Figure 3 reports only the median target impulse responses for both the linear and the nonlinear VARs. A few facts stand out. First, there is evidence of a negative response of all real activity indicators to an uncertainty shock according to both models. Looking at the identified set, real activity indicators go down on impact after an uncertainty shock according to the large majority of retained models. This evidence is stronger for the great recession case. The responses during the great recession are substantially larger than those in normal times. This is true despite of the close similarity between the response of uncertainty in the two states we consider. This latter evidence points to a different transmission mechanism at work in normal times vs. during an extreme event as the great recession. The next Section will dig deeper and seek for the structural explanation behind these different responses. Table 2 reports the peak response of output during the great recession. Notably, it is about 50% larger than the average response. The same indication comes from consumption, whose peak reaction is 32% larger in great recession, and even more so for investment and hours, whose peak responses during the great recession are two and a half and two times larger than average, respectively. Third, the response of real activity indicators is more persistent during the great recession. Fourth, the response of the policy rate is negative and persistent according to both models, while that of the price level is negative during the great recession, and negligible in the linear case.

Are these responses different from a statistical standpoint? Figure 4 shows the out-

[13] The number of accepted draws is about 0.2% for both the linear VAR and the IVAR. More precisely, out of one million, we retain 2,116 draws for the linear VAR, and 2,168 for the IVAR. Following Fry and Pagan (2011), the median target (MT) response is produced by considering the unique retained model whose implied impulse responses are the closest to the median responses (across models) over the horizon we consider.

come of the bootstrapped test for the difference of the median target responses between the great recession and normal times, along with the 90% confidence bands.[14] As evident from the figure, the responses of output, investment, and hours are significantly larger in recessions, an evidence which offers statistical support to the more pronounced macroeconomic responses during the great recession discussed above. The reaction of consumption is only borderline significant, with the mass of the distribution which however hints to a larger response in the great recession. Finally, also the response of the price level and the nominal interest rate is found to be significantly different between the two states.[15]

Overall, these results point to an economically and significantly stronger response of real activity to an uncertainty shock in an extreme event like the great recession. To interpret this fact, we turn to the use of a structural model in the next Section.

4 Uncertainty-driven contractions: A structural interpretation

4.1 DSGE model: Description and estimation

Description. The Basu and Bundick (2017) framework extends an otherwise standard New Keynesian model to consider an ex-ante second moment shock in the preference shock process, which has got a direct influence on a well-defined ex-ante financial volatility concept within the model. We briefly describe the model here, focusing on the parts that are crucial for our study. We refer the reader to Basu and Bundick's (2017) paper for further details.

Households work, consume, and invest in equity shares and one-period risk-free

[14] For each variable, the figure is based on the distribution constructed by considering 1,000 differences between responses in the linear model and responses obtained from the IVAR for the great recession. Such responses are generated from 1,000 samples obtained via the standard residual-based bootstrap around the median target responses. For each sample, we estimate the IVAR and nested linear VAR, compute the corresponding GIRFs and IRFs, and take their difference. The 90% confidence bands are constructed by considering the point estimate of the impulse responses ± 1.64 times the bootstrapped estimate of the standard errors. The construction of the test statistic takes into account the correlation between the estimated impulse responses. Our Appendix shows that the difference in the responses holds true also when model uncertainty is accounted for.

[15] Obviously, the great recession was characterized by a combination of first-moment financial shocks and uncertainty shocks (Stock and Watson (2012)). Our Appendix documents an exercise in which we model the BAA-AAA spread along with the other variables of our VAR, and we implement an event-based approach to separately identify first and second-moment financial disturbances. The impulse responses obtained with this expanded vector of variables are pretty close to the ones documented here.

bonds. They are all similar, and feature Epstein-Zin preferences over streams of consumption and leisure, formalized as follows:

$$V_t = \left[\left(1-\beta)(a_t \tilde{C}_t^{\eta}(1-N_{t,})^{(1-\eta)} \right)^{(1-\sigma)/\theta_V} + \beta((E_t V_{t+1})^{1-\sigma})^{1/\theta_V} \right]^{\theta_V/(1-\sigma)}$$

where $\tilde{C}_t = C_t - H_t$, C_t is consumption, $H_t = bC_{t-1}$ captures external habit formation in consumption related to the level of aggregate consumption lagged one period, N_t is hours worked, β is the discount factor, σ is a parameter directly influencing the degree of risk aversion, ψ is the intertemporal elasticity of substitution, $\theta_V \equiv (1-\sigma)/(1-\psi^{-1})^{-1}$ captures households' preferences for the resolution of uncertainty, η weights consumption and labor in households' happiness function, and a_t is a stochastic shifter influencing the relevance of today's realizations of consumption and labor vs. those expected to occur during the next period.[16]

The stochastic process followed by this preference shock is:

$$\begin{aligned} a_t &= (1-\rho_a)a + \rho_a a_{t-1} + \sigma_{t-1}^a \varepsilon_t^a \\ \sigma_t^a &= (1-\rho_{\sigma^a})\sigma^a + \rho_{\sigma^a}\sigma_{t-1}^a + \sigma^{\sigma^a}\varepsilon_t^{\sigma^a} \end{aligned}$$

where ε_t^a is the first-moment preference shock, and $\varepsilon_t^{\sigma^a}$ is a second-moment uncertainty shock to the preference process which loads the law of motion regulating the evolution of the time-varying second moment σ_t^a relative to the distribution of ε_t^a. With respect to the framework in Basu and Bundick (2017), we add (external) habit formation in consumption to capture the hump-shaped response of consumption in the data (for another contribution jointly modeling Epstein-Zin preferences and habits in consumption, see Andreasen, Fernández-Villaverde, and Rubio-Ramírez (2018)).

Intermediate goods-producing firms operate in a monopolistically competitive environment, rent labor from households, and pay wages. They own capital and choose its utilization rate, issue equity shares and one-period riskless bonds, and invest in physical capital to maximize the discounted stream of their profits. In doing so, they face quadratic costs of adjusting nominal prices à la Rotemberg (1982), capital adjustment costs à la Jermann (1998), and capital utilization costs influencing the capital depreciation rate. All intermediate firms have the same Cobb-Douglas production function, and

[16] de Groot, Richter, and Throckmorton (2018) show that households' preferences in Basu and Bundick's (2017) paper imply an asymptote in the responses to an uncertainty shock with unit intertemporal elasticity of substitution. Our paper employs the set of preferences proposed by Basu and Bundick (2018), which do not imply any asymptote.

are subject to a fixed cost of production and stationary technology shocks. Intermediate goods are packed by a representative final goods producer operating in a perfectly competitive market. The model is closed by assuming that the central bank follows a standard Taylor rule, which reads as follows:

$$r_t = r + \rho_\pi(\pi_t - \pi) + \rho_y \Delta y_t$$

where $r_t = \ln(R_t)$, $\pi_t = \ln(\Pi_t)$, $\Delta y_t = \ln(Y_t/Y_{t-1})$, R_t is the gross nominal interest rate, Π_t is gross inflation, π is the net inflation target, and Y_t is output. Hence, monetary policymakers are assumed to systematically respond to changes in inflation and the growth rate of output.

In this framework, an uncertainty shock propagates to the economy mainly via precautionary savings and precautionary labor supply.[17] The former effect reduces current consumption in response to an increase in uncertainty, while the latter increases labor supply, which drives real wages and firms' marginal costs down. Given that prices are sticky, the price markup increases. Output, which is demand-driven in this model, falls due to the drop in consumption, and labor demand contracts driving hours down. Given the lower return on capital, investment falls too. Hence, in equilibrium, an increase in uncertainty causes a drop in all four real activity indicators, i.e., output, consumption, investment, and hours, which is what we observe in the data.

As anticipated above, the model features a well-defined implied financial volatility index. This is because intermediate firms issue equity shares on top of one-period riskless bonds.[18] Each equity share has a price P_t^E and pays dividends D_t^E, implying a one-period return $R_{t+1}^E = \left(P_{t+1}^E + D_{t+1}^E\right)/P_t^E$. The model-implied financial uncertainty index V_t^M is computed as the annualized expected volatility of equity returns, i.e., $V_t^M = 100\sqrt{4 \cdot VAR_t\left(R_{t+1}^E\right)}$, where $VAR_t\left(R_{t+1}^E\right)$ is the quarterly conditional variance

[17] Given that adjustment costs are convex, this model does not imply a "wait-and-see" effect after an uncertainty shock. The reason is that, to solve the model, we use perturbation methods which require policy functions to be differentiable, a feature which is not possessed by threshold policy functions arising in presence of real option effects. Still, investment potentially matters for the propagation of uncertainty shocks through the two channels explained in Bianchi, Kung, and Tirskikh (2019), i.e., an investment risk premium channel, which depends on the covariance between the pricing kernel and the return on investment, and a investment adjustment channel, which arises because of rigidities which prevent firms to immediately adjust investment to the desired level.

[18] Basu and Bundick (2017) assume that firms finance a share ν of their capital stock each period with one-period riskless bonds. Given that the Modigliani-Miller theorem holds in their model, leverage does neither influence firms' value nor firms' optimal decisions. Firms' leverage only influences the first two unconditional moments of financial-related quantities (e.g., the average level and unconditional volatility of the model-implied VXO and the equity premium), but it does not influences impulse responses to an uncertainty shock.

of the return on equity R^E_{t+1}. Equity returns are endogenous in the model, which makes V^M_t endogenous too. However, in this model V^M_t is almost entirely driven by second-moment preference shocks for a variety of plausible calibrations. This enables us to treat the uncertainty shock as a financial uncertainty shock proxied by V^M_t, with a clear empirical counterpart, which justifies why we can use the facts established with the VAR to estimate the DSGE model.[19]

We work with a third-order approximation of the nonlinear DSGE model, which we solve via perturbation techniques (Schmitt-Grohe and Uribe (2004)). The third order approximation of agents' decision rules features an independent role for uncertainty, whose independent effect on the equilibrium values of the endogenous variables of the framework can therefore be studied (Andreasen (2012)). Perturbation represents an accurate and fast way to find a solution also working with frameworks featuring recursive preferences (Caldara, Fernández-Villaverde, Rubio-Ramírez, and Yao (2012)).

Estimation. We estimate the model described above via the impulse response function-matching approach popularized by Christiano, Trabandt, and Walentin (2011). In particular, we employ a Bayesian approach via which we impose economically sensible prior densities on the structural parameters while asking the data (i.e., our IVAR impulse responses) to shape the posterior density of the estimated model. With respect to Christiano, Trabandt, and Walentin (2011), who focus on a linearized DSGE framework and a linear VAR as auxiliary model, we estimate a nonlinear DSGE framework approximated at a third order with moments produced with a linear VAR on the one hand, and an Interacted VAR on the other.[20] Further details of our minimum-distance estimation strategy are reported in our Appendix.

We estimate 7 structural parameters, i.e. $\boldsymbol{\zeta}^i = \left[\rho_{\sigma^a}, \sigma, b, \phi_K, \phi_P, \rho_\pi, \rho_y\right]$. These parameters are the persistence of the second moment preference shock ρ_{σ^a}, the household risk aversion parameter σ, the consumption habit formation parameter b, the parameter regulating investment adjustment costs ϕ_K, the parameter regulating price adjustment costs ϕ_P, and the parameters of the Taylor rule ρ_π, ρ_y. Our priors are reported in the

[19] A Monte Carlo simulation documented in our Appendix shows that the Narrative Sign Restrictions we work with to identify uncertainty shocks from the VXO is able to recover the "true" responses produced by the DSGE model.

[20] One way of interpreting this exercise is to think of a regime-switching type of estimation in which we allow the parameters of the nonlinear DSGE model to be state-dependent. Bianchi and Melosi (2017) formally model policy-related uncertainty with a regime-switching approach which allows agents to formulate a prediction over future regime switches in an empirical framework where the DSGE model is a linearized framework within each state. A challenge for future research is how to conduct such an exercise with a nonlinear DSGE model like the one we work with.

third column of Table 3. We calibrate the prior means with the values in Basu and Bundick's (2017) analysis, and we use diffuse priors. For the habit formation parameter and the parameters of the Taylor rule, we use the priors employed by Christiano, Trabandt, and Walentin (2011).[21] The remaining parameters of the model are calibrated as in Basu and Bundick (2018). We discuss the calibration of these parameters in our Appendix.

4.2 Linear versus great recession-specific estimation results

Our DSGE model-based estimated responses are reported in Figure 5, along with the VAR-based bootstrapped confidence bands.[22] The model captures remarkably well the VAR dynamics both in normal times and during the great recession. Most of the DSGE impulse responses lie within the 90% confidence bands of the IVAR impulse responses. Moreover, it clearly works well quantitatively for output (as well as consumption and investment), which will be the target of our investigation on the role of monetary policy during extreme events we will entertain later. Figure 6 focuses on the responses implied by the two estimated versions of the DSGE framework (normal times. vs great recession). The model clearly generates a stronger response of all real activity indicators during the great recessions than in normal times. Turning to the nominal side, the model is able to capture the more marked response of prices during the great recession, and replicates by and large the expansionary monetary policy responses in both scenarios.[23]

[21] Canova and Sala (2009) show that the use of priors can hide identification issues even in population when it comes to estimating linearized DSGE frameworks. Given that we use priors common to the two regimes we focus on, lack of identification would work against finding state-dependent parameter estimates. We anticipate that our results point to substantial differences in the parameter estimates between regimes. An exercise dealing with identification issues in the estimation of nonlinear DSGE frameworks is material for future research.

[22] Our bootstrapped confidence bands are based over 1,000 realizations for the impulse responses, which are used to compute the bootstrapped estimate of the standard errors of the impulse response functions. As in Altig, Christiano, Eichenbaum, and Lindé (2011), the 90% confidence bands are constructed by considering the median target point estimates of the impulse response ± 1.64 times the bootstrapped estimate of the standard errors.

[23] The model is less successful in replicating the magnitude of the drop in hours worked during the great recession, a result we share with Basu and Bundick (2017). Possible explanations are: i) the assumption of homogeneous workers, which misses to take into account differences the relatively faster exit from the labor market by unskilled workers during recessions (for a discussion, see Basu and Bundick (2017)); ii) the role played by the precautionary labor supply channel, which leads to an increase in labor supply under uncertainty and dampens the magnitude of the drop in hours worked in equilibrium (Bianchi, Kung, and Tirskikh (2019)); iii) the absence of search frictions, which can magnify the real effects of uncertainty shocks (Leduc and Liu (2016)), above all if combined with an occasionally binding constraint on downward wage adjustment (Cacciatore and Ravenna (2018)). However, our model is able to replicate the fall in output to an uncertainty shock, which is the dynamic

Table 3 collects the estimated parameters of the DSGE model for both regimes. In spite of sharing the same priors, some of the estimated parameters are clearly state-dependent. In particular, households' risk aversion is estimated to be larger during the great recession; prices are found to be stickier during the great recession; while investment adjustment costs are estimated to be higher. On the other hand, both the degree of habits in consumption and the persistence of the second moment preference shock ρ_{σ^a} are estimated to be the same between states. The latter implies that the different effects of uncertainty shocks in model-based responses are fully due to a different propagation mechanism which is only explained by differences in structural parameters.[24] This evidence is in line with our VAR-related findings on the larger responses during the great moderation in spite of a similar (statistically equivalent) dynamic path of financial uncertainty in the two states under scrutiny. Finally, the estimated policy rule points to a similar response to inflation and a stronger reaction to output during the great recession.

4.3 Parameter instability

Which are the parameters behind the stronger response of real activity to an uncertainty shock during the great recession? To address this question, we conduct a sensitivity analysis (reported in our Appendix for the sake of brevity) via which we check the impact of parameter estimates on the impulse responses of our estimated DSGE framework. We find three parameters to be behind the larger real activity response during the great recession: the degree of risk aversion, investment adjustment costs; and the monetary policy response to output growth.[25]

Risk aversion is found to be larger during the great recession. As explained by Swanson (2012), the coefficient of relative risk aversion in this type of models is affected

response we focus on in the policy-related part of our analysis. We leave an extension of our analysis with a model of the labor market suited to capture the response of aggregate hours to an uncertainty shock to future research.

[24] Breaks in structural parameters in DSGE frameworks are also detected by, among others, Fernández-Villaverde and Rubio-Ramírez (2008), Canova (2009), and Inoue and Rossi (2011). With respect to these analyses, our investigation focuses on the changes related to moving from normal times to the great recession.

[25] Our Appendix also documents the irrelevance of initial conditions for our DSGE results. Cacciatore and Ravenna (2018) prove that pruning completely eliminates state dependence in the propagation of uncertainty shocks from third-order approximated solutions. Hence, the unpruned solution of the model may in principle generate state-dependent dynamics. However, an IVAR estimated with data simulated from the unpruned approximated solution of our estimated model turns out to deliver impulse responses that are quantitatively insensitive to variations in the initial conditions.

by the labor market structure as well as households' preference. Building on Swanson (2012), Swanson (2018) works out the expression for the coefficient of relative risk aversion conditional on endogenous labor supply, habits in consumption, and generalized recursive preferences (which include Epstein-Zin preferences). Following Swanson (2018), our estimated parameters imply a coefficient of relative risk aversion equal to 105 in the linear case, and 145 in great recession (see Table 3).[26] These values are in the ballpark of the calibrated (75) and estimated (110) ones in Rudebusch and Swanson (2012) (a paper whose goal is not that of matching moments during extreme events), but are higher than those typically used in the macroeconomic literature. A possible reason is the lack of model uncertainty in our framework. Barillas, Hansen, and Sargent (2009) employ a max-min expected utility theory approach to show that models with high risk aversion in which rational agents are endowed with the knowledge of the true underlying structure of the economy can be reinterpreted as frameworks in which risk aversion is low but households have doubts about the model specification. Our model does not embed any doubts about the underlying economy by households. Therefore, it is likely to understate the true quantity of risk faced by households in the data, which is the reason why it requires high levels or risk aversion to match the VAR facts.[27] Our finding of a higher risk aversion is in line with Cochrane (2017), who points out that a countercyclical risk aversion is a feature macro-finance models should possess to match the data; Cohn, Engelmann, Fehr, and Maréchal (2015), who provide experimental evidence suggesting that financial market professionals are more risk averse during a financial bust than a boom; Guiso, Sapienza, and Zingales (2017), who propose experimental evidence in favor of a fear model in which agents experience higher risk aversion in periods of crisis; and Schildberg-Horisch (2018), who surveys the literature on risk aversion and finds that, for negative economic shocks such as the

[26] The formula for the RRA in our extension of the Basu and Bundick (2017) model with habits takes the following form (see our Appendix for the full derivation):

$$RRA = \left(\frac{\eta}{\eta + (1-\eta)(1-b)}\right) \cdot \left(\frac{1}{\psi}\frac{\left(1 + \frac{(1-\eta)}{\eta}(1-b)\right)}{(1-b)\left(1 + \frac{(1-\eta)}{\eta}\right)} + \left(\sigma - \frac{1}{\psi}\right)\left(\frac{\eta}{(1-b)} + 1 - \eta\right)\right)$$

[27] Andreasen, Fernández-Villaverde, and Rubio-Ramírez (2018) show that, in a model featuring a portfolio allocation problem related to short- and long-term bonds plus a systematic response of the central bank to the term spread, uncertainty shocks to households' preferences generate moments consistent with the data even in presence of moderate values of risk aversion. The moments studied by Andreasen, Fernández-Villaverde, and Rubio-Ramírez (2018) are, however, unconditional moments, i.e., they are not state-specific.

2007-09 financial crisis, the evidence consistently points to an increase in risk aversion.

Turning to investment adjustment costs, we find them to be larger during the great recession. The role played by adjustment costs of investment in magnifying the response of investment to an uncertainty shock is well explained by Basu and Bundick (2017). In this model, investment adjustment costs make it more difficult for households to convert their desired savings into physical assets. Hence, large(r) adjustment costs can work in favor of magnifying the reaction of investment to a jump in uncertainty.[28] Our evidence lines up with that in Lanteri (2018) and Dibiasi (2018), who propose evidence consistent with a countercyclical degree of reallocation frictions.

Finally, we estimate a larger monetary policy response to output growth during the great recession. This estimate captures the rapid and massive interventions by the Federal Reserve in response of the dramatic drop in real activity occurred in 2008-09. This intuitive interpretation is supported by policy statements on the importance of contrasting the negative pressures on real activity in that period.[29]

4.4 Monetary policy and output loss during the great recession

Equipped with the DSGE model estimated using the great recession-specific impulse responses, we now turn to the analysis of the role played by monetary policy in the propagation of the 2008Q4 uncertainty shocks. Table 3 documents a more aggressive systematic response to output growth during the great recession (the parameter attached to output in the DSGE policy rule is 0.28 for the great recession, compared with 0.20 in normal times). A natural question is whether such a more aggressive response of the Fed helped mitigate the depth of the great recession. To address this question, we take our DSGE model with the parameters set at their estimated values for the great recession (see Table 3, column 5). We then replace the estimated parameter in the policy rule attached to output with the value of the same parameter obtained in normal times, i.e., we replace $\rho_y^{GR} = 0.28$ with $\rho_y^{linear} = 0.20$. We then generate the corresponding GIRF to a 4.4 standard deviation uncertainty shock. Figure 7 presents the results. The counterfactual fall in output would have been roughly doubled in 2008Q4

[28] To be sure, too large investment adjustment costs would actually work in the opposite direction, in that they would prevent firms from disinvesting, and large drop in real activity to occur.

[29] See, for instance, the minutes of the Federal Open Market Committee meeting held on October 28-29, 2008, where all FOMC members *"[...] judged that a significant easing in policy at this time was appropriate to foster moderate economic growth and to reduce the downside risks to economic activity."* After that meeting, the federal funds rate target was cut by 50 basis points.

and the recession would have been longer, lasting until the second half of 2010. Hence, according to our estimated framework, the Fed played a significant role in mitigating the depth of the great recession.[30]

5 Covid-19-induced uncertainty shock: Output loss and monetary policy

5.1 Output loss in three different scenarios

The Covid-19 outbreak generated an unprecedented increase in the level of uncertainty, with the all-time high value of the VIX of 82.69 recorded on March 16 surpassing the 80.06 reached on October 27, 2008. Similar to what happened in 2008 between the third and fourth quarter, the increase of the VIX in March 2020 was fivefold compared with the previous quarter. What are the business cycle consequences of such a large uncertainty shock? We address this question by employing the DSGE model estimated with great recession data as a laboratory.[31] Based on the information set available to economic agents in the first quarter of 2020, we then simulate the effects of the uncertainty shock due to Covid-19 allowing for the possibility of experiencing a second wave of the pandemic in the future. In the context of our DSGE model, this translates to allowing for an anticipated uncertainty shock. Hence, we modify the baseline stochastic

[30] Two things are worth noticing. First, our DSGE model accounts only for conventional monetary policy intervention. However, the federal funds rate was 1.94% in 2008Q3. Hence, in principle, the Fed had enough space to intervene, at least in the short run, i.e., before hitting the ZLB in December 2008 (or before 2009Q1 according to our quarterly model). Second, according to the estimation of our IVAR it was the interaction of uncertainty shocks and other shocks (possibly financial shocks) that brought the economy at the ZLB. Indeed, our results in figure 3 show that, even when using the shadow rate (which can turn negative), our IVAR does not suggest that the response of the Fed to the uncertainty shock of 2008Q4 *alone* was sufficient to "break" the ZLB. This means that a DSGE model estimated on the basis of our great recession IVAR response is in principle able to capture the aggressiveness of the Fed response to the 2008Q4 uncertainty shock.

[31] This great recession-Covid-19 pandemic parallel is obviously to be taken with a grain of salt. There are profound differences between the mechanics of the two recessions (first and foremost, the absence of a lockdown during the great recession, which has enormously contributed to the output loss associated to the Covid-19 recession). On the other hand, similarities between the two recessions can also be drawn. First, the jump in financial uncertainty at the beginning of the two recessions has been quantitatively similar. Second, available estimates of the risk aversion in these two recessions point to a similar jump (Bekaert, Engstrom, and Xu (2019)). Third, as pointed out in the following sub-Section, the magnitude of the cut in the federal funds rate during the quarter after the uncertainty shock in both recession is comparable, and can arguably be attributed to a switch to a relatively more aggressive output stabilization policy.

process for the preference shock as follows:

$$\begin{aligned} a_t &= (1-\rho_a)\, a + \rho_a a_{t-1} + \sigma^a_{t-1}\varepsilon^a_t \\ \sigma^a_t &= (1-\rho_{\sigma^a})\sigma^a + \rho_{\sigma^a}\sigma^a_{t-1} + \sigma^{\sigma^a}\varepsilon^{\sigma^a}_t + \sigma^{\sigma^a}_n \varepsilon^{\sigma^a}_{t-j}. \end{aligned}$$

where $\varepsilon^{\sigma^a}_{t-j}$ represents the anticipated second moment shock (with anticipation horizon j), and $\sigma^{\sigma^a}_n$ is the volatility of such a shock. Similarly to the unanticipated one, the anticipated volatility shock is assumed to be a white noise.

To simulate our model with the above described structure for the uncertainty shock, we need to calibrate the anticipation horizon j, the standard deviations of the unanticipated and anticipated shock - respectively, σ^{σ^a} and $\sigma^{\sigma^a}_n$ -, the size (in terms of standard deviations) of the unanticipated and the anticipated shocks, $\varepsilon^{\sigma^a}_t$ and $\varepsilon^{\sigma^a}_{t-j}$, respectively, the persistence of the preference shock ρ_a and that of the uncertainty process ρ_{σ^a}, and the steady state volatility σ^a.

To calibrate the size of the unexpected uncertainty shock, we observe that the increase in our modelled VXO (in log) between 2008Q3 and 2008Q4 is similar to that observed between 2019Q4 and 2020Q1: they correspond, respectively, to a percent increase in the VXO of 129% and 133%. Based on this observation, we calibrate the size of the uncertainty shock in 2020Q1 exactly in line with that of 2008Q4, i.e. equal to 4.4 standard deviations. Moreover, we borrow the steady state volatility and the persistence of the preference and volatility processes from the estimates and calibration of the great recession model. We then set the standard deviation of the anticipated uncertainty shock to be 75% the level of the standard deviation of the unanticipated component: $\sigma^{\sigma^a}_n = 0.75\sigma^{\sigma^a} = 0.003$. The idea is that of acknowledging that, while one the one hand uncertainty is still expected to be present in Fall 2020 (e.g., the massive use of effective vaccines will most likely not be available yet), on the other hand the scientific community has certainly gained knowledge about the pandemic since March 2020 (e.g., some drugs have reduced mortality rates and recovery times).[32] Hence, the amount of Covid-19-related uncertainty is likely to be lower, although still relatively high. Conditional on this calibration, we construct the following three different scenarios characterized by different sizes of a second wave-related uncertainty shock:

i) an "optimistic" one, characterized by the absence of the anticipated uncertainty shock, i.e., $\varepsilon^{\sigma^a}_{t-j} = 0$ per each possible j. In other words, this scenario just admits the

[32] See, e.g., Dr. Anthony Fauci's interventions here: https://www.mercurynews.com/2020/07/10/fauci-everything-we-know-about-covid-19-so-far/ , and here: https://www.youtube.com/watch?v=ybZjaINKZ-8 .

contemporaneous unexpected uncertainty shock, and does not allow for any "second wave" shock;

ii) an "intermediate" one, which features $j = 2$ (i.e., it assumes a second wave in the Fall of 2020, as expected by households in March 2020), and a size of the anticipated shock which is 75% that of the unanticipated component in 2020Q1, i.e., 3.3 $(0.75 \cdot 4.4)$ standard deviations. This calibration is justified by statements made in March 2020 by experts in the medical field about the likelihood of a second wave in the Fall of 2020;[33]

iii) a "pessimistic" scenario, which still features $j = 2$, but it assumes the anticipated uncertainty shock in 2020Q3 to feature 150% the size of the unexpected one that hit in 2020Q1, i.e., 6.6 $(1.5 \cdot 4.4)$ standard deviations. This calibration is in line with the evidence of the first two waves of the Spanish flu in 1918.[34]

Figure 8 (left panel) reports the impulse responses for the three Covid-19 scenarios, while Table 4 collects the peak and cumulative responses of our real activity indicators and contrasts them with the figures related to the great recession.[35] The optimistic scenario replicates (by construction) the outcome of the great recession, which we briefly comment here once again. Output reaches its trough after five quarters, falling by -2.5 percentage points compared to the pre-shock level. Under this scenario, the cumulative loss (i.e., the integral of the output response) amounts to -35.2%. Turning to the other two scenarios, the effect of the expected second wave in 2020Q3 is evident, with a deeper and longer recession predicted by our framework. As documented in Table 4, all real activity indicators fall by a larger amount. In the pessimistic scenario, output reaches a peak drop of -6.5% after six quarters, more than twice the peak drop estimated for the great recession. The recession is absorbed at a much slower pace, and the cumulative loss is more than twice and 1/2 as large as that experienced after the great recession (-92.6% compared with -35.2%). Also in the intermediate scenario, the recession caused

[33] In a recent interview on April 1 2020, Yale University Professor Nicholas Christakis (MD, PhD, MPH) states that in Fall 2020 the US will have a 75% chance of getting a second wave of the pandemic (the podcast by the Journal of American Medical Association (JAMA) Network is available at https://edhub.ama-assn.org/jn-learning/audio-player/18393767; around 25').

[34] See https://en.wikipedia.org/wiki/Spanish_flu#Deadly_second_wave_of_late_1918 . To our knowledge, Barro, Ursúa, and Weng (2020) were the first ones to draw a parallel between the 1920 Spanish flu and the 2020 coronavirus pandemic, and to study the economic implications of these two events.

[35] The impulse responses are constructed in the same way as explained in Section 4, the only difference being that in this case we hit the system with two shocks, the unexpected uncertainty shock and the expected uncertainty news shock. Notice that the findings of Cacciatore and Ravenna (2018) imply that one can sum the two separate GIRFs obtained for each shock taken in isolation, as in a third-order perturbation with pruning uncertainty shocks propagate linearly. Our simulations, not reported but available upon request, show that this is indeed the case for our model.

by the Covid-19 outbreak is expected to induce a deeper recession compared with the great recession, with a peak drop in output of -4.5 percentage points, and a cumulative loss of -63.4%.

5.2 The role of monetary policy

A similarity between the great recession and the Covid-19 outbreak has been the prompt and massive response of the Federal Reserve in terms of policy rate cut. In 2008, the federal funds target rate dropped by 175 basis points over one quarter, from a level of 2% in September to 0.25% in December. In 2020, the federal funds target range dropped by 150 basis points over the same time span, moving from a range of 1.75%-1.5% in December 2019 to a range of 0.25-0% in March 2020. We take this evidence as supportive of a switch toward an aggressive response to the drop in output in the aftermath of the Covid-19 shock. How deeper would the Covid-19-induced recession be if the Fed followed a "business as usual" type of conduct? We answer this question by recomputing the impulse responses in the three scenarios previously described by substituting the estimate of the response to output in the Taylor rule conditional on great recession data ($\rho_y = 0.28$) with that estimated for "normal times" ($\rho_y = 0.2$).

Figure 8 (right panel) reports the so-obtained counterfactual impulse responses. A milder response of the Fed to output would cause a deeper recession, with a drop in output about 50% larger. Looking at the pessimistic scenario, output would have dropped from an estimated peak of -6% to -9% under the (counterfactual) "normal times" monetary policy. Our simulations suggest that the implied drop in the interest rate would be milder (-2%, as opposed to -2.5% under the more aggressive output stabilization policy), with a much slower return to the pre-shock output level.

6 Conclusion

This paper documents the output costs due to uncertainty shocks during extreme events such as the great and the Covid-19 recessions. We employ a nonlinear VAR and a state-of-the-art identification strategy to estimate the response of real activity to a financial uncertainty shock in normal times vs. the great recession. We find a substantially larger response of a battery of business cycle indicators to an uncertainty shock during the great recession. We then use this evidence to estimate a nonlinear DSGE framework which features a time-varying financial volatility concept comparable to the one modeled with our VAR. The DSGE model is estimated in a state-dependent fashion, i.e., using

facts related to normal times and to the great recession. We find a stronger policy response to output growth to be supported by the data during the great recession, along with higher risk aversion and investment adjustment costs.

We then use our estimated framework to conduct counterfactual simulations to quantify the impact of the aggressive monetary policy implemented by the Federal Reserve during the great recession. We find that such an aggressive policy halved the cumulative output loss which would have otherwise materialized, and shortened the duration of the recession. Finally, we use the model estimated with great recession data as a proxy of the US economy during the Covid-19 pandemic (lockdown apart). With such model, we simulate different scenarios each of which is characterized by a different path of expected financial uncertainty in the quarters after the Covid-19 uncertainty shock. These scenarios differ because of the different weight we assign to a second wave of the pandemic in Fall 2020 as expected by agents in March 2020. We find that the cumulative output loss could eventually be three times as large as the one implied by the model during the great recession. As for the great recession, an aggressive monetary policy is associated to a dramatic reduction in the output loss that would otherwise arise if systematic monetary policy were conducted in a "normal times" fashion.

Our findings support the switch to an aggressive, relatively more output stabilization-focused monetary policy during extreme events characterized by large uncertainty shocks. From a modeling standpoint, our results support Greenspan's quote reported at the beginning of the paper on the need of using nonlinear frameworks to model aberrations in the data.

References

Alessandri, P., and H. Mumtaz (2019): "Financial Regimes and Uncertainty Shocks," *Journal of Monetary Economics*, 101, 31–46.

Altig, D., L. J. Christiano, M. Eichenbaum, and J. Lindé (2011): "Firm-Specific Capital, Nominal Rigidities and the Business Cycle," *Review of Economic Dynamics*, 14(2), 225–247.

Andreasen, M. M. (2012): "On the Effects of Rare Disasters and Uncertainty Shocks for Risk Premia in Non-Linear DSGE Models," *Review of Economic Dynamics*, 15(3), 295–316.

Andreasen, M. M., J. Fernández-Villaverde, and J. F. Rubio-Ramírez (2018): "The Pruned State-Space System for Non-Linear DSGE Models: Theory and Empirical Applications," *Review of Economic Studies*, 85(1), 1–49.

Angelini, G., E. Bacchiocchi, G. Caggiano, and L. Fanelli (2019): "Uncertainty Across Volatility Regimes," *Journal of Applied Econometrics*, 34(3), 437–455.

Antolín-Díaz, J., and J. F. Rubio-Ramírez (2019): "Narrative Sign Restrictions," *American Economic Review*, forthcoming.

Baker, S., N. Bloom, S. J. Davis, and S. J. Terry (2020): "COVID-Induced Economic Uncertainty," available at https://nbloom.people.stanford.edu/.

Baker, S., N. Bloom, and S. J. Terry (2020): "Does Uncertainty Reduce Growth? Using Disasters As Natural Experiments," available at https://nbloom.people.stanford.edu/research.

Barillas, F., L. P. Hansen, and T. J. Sargent (2009): "Doubts or Variability?," *Journal of Economic Theory*, 144, 2388–2418.

Barro, R., J. Ursúa, and J. Weng (2020): "The Coronavirus and the Great Influenza Pandemic. Lessons from the "Spanish Flu" for the Coronavirus's Potential Effects on Mortality and Economic Activity," NBER Working Paper No. 26866.

Basu, S., and B. Bundick (2017): "Uncertainty Shocks in a Model of Effective Demand," *Econometrica*, 85(3), 937–958.

Basu, S., and B. Bundick (2018): "Uncertainty Shocks in a Model of Effective Demand: Reply," *Econometrica*, 86(4), 1527–1531.

Bekaert, G., E. Engstrom, and N. R. Xu (2019): "The Time Variation in Risk Appetite and Uncertainty," Columbia Business School Research Paper No. 17-108.

Bianchi, F., H. Kung, and M. Tirskikh (2019): "The Origins and Effects of Macroeconomic Uncertainty," Duke University and London Business School, mimeo.

Bianchi, F., and L. Melosi (2017): "Escaping the Great Recession," *American Economic Review*, 107(4), 1030–58.

Bloom, N. (2009): "The Impact of Uncertainty Shocks," *Econometrica*, 77(3), 623–685.

Bretscher, L., A. Hsu, and A. Tamoni (2018): "Risk Aversion and the Response of theMacroeconomy to Uncertainty Shocks," London Business School, Georgia University of Technology, and London School of Economics, mimeo.

Cacciatore, M., and F. Ravenna (2018): "Uncertainty, Wages, and the Business Cycle," HEC Montreal, mimeo.

Caggiano, G., E. Castelnuovo, and N. Groshenny (2014): "Uncertainty Shocks and Unemployment Dynamics: An Analysis of Post-WWII U.S. Recessions," *Journal of Monetary Economics*, 67, 78–92.

Caggiano, G., E. Castelnuovo, and G. Pellegrino (2017): "Estimating the Real Effects of Uncertainty Shocks at the Zero Lower Bound," *European Economic Review*, 100, 257–272.

Caldara, D., J. Fernández-Villaverde, J. F. Rubio-Ramírez, and W. Yao (2012): "Computing DSGE Models with Recursive Preferences and Stochastic Volatility," *Review of Economic Dynamics*, 15, 188–206.

Canova, F. (2009): "What Explains the Great Moderation in the US? A Structural Analysis," *Journal of the European Economic Association*, 7(4), 697–721.

Canova, F., and L. Sala (2009): "Back to Square One: Identification Issues in DSGE Models," *Journal of Monetary Economics*, 56(4), 431–449.

Christiano, L., M. Trabandt, and K. Walentin (2010): "DSGE Models for Monetary Policy Analysis," in B. M. Friedman and M. Woodford (editors): Handbook of Monetary Economics, Volume 3a, Chapter 7, 285-367, Elsevier B.V., North-Holland.

Christiano, L., M. Trabandt, and K. Walentin (2011): "DSGE Models for Monetary Policy Analysis," in: B. M. Friedman and M. Woodford (Eds.): Handbook of Monetary Economics, Volume 3a, 285–367.

Cochrane, J. (2017): "Macro-Finance," *Review of Finance*, 21(3), 945–985.

Cohn, A., J. Engelmann, E. Fehr, and M. A. Maréchal (2015): "Evidence for Countercyclical Risk Aversion: An Experiment with Financial Professionals," *American Economic Review*, 105(2), 860–885.

de Groot, O., A. W. Richter, and N. A. Throckmorton (2018): "Uncertainty Shocks in a Model of Effective Demand: Comment," *Econometrica*, 86(4), 1513–1526.

Dibiasi, A. (2018): "Non-linear Effects of Uncertainty," KOF ETH Zurich Swiss Economic Institute, mimeo.

Fernández-Villaverde, J., and J. Rubio-Ramírez (2008): "How Structural are Structural Parameters?," in (Eds.) D. Acemoglu, K. Rogoff, and M. Woodford: NBER Macroeconomics Annual, Vol. 22, 83–137.

Fry, R., and A. Pagan (2011): "Sign Restrictions in Structural Vector Autoregressions: A Critical Review," *Journal of Economic Literature*, 49(4), 938–960.

Greenspan, A. (2003): "Monetary Policy under Uncertainty," Remarks at a symposium sponsored by the Federal Reserve Bank of Kansas City, Jackson Hole, Wyoming, August 29.

Guiso, L., P. Sapienza, and L. Zingales (2017): "Time Varying Risk Aversion," *Journal of Financial Economics*, forthcoming.

Inoue, A., and B. Rossi (2011): "Identifying the Sources of Instabilities in Macroeconomic Fluctuations," *Review of Economics and Statistics*, 93(4), 1186–1204.

Jermann, U. (1998): "Asset Pricing in Production Economies," *Journal of Monetary Economics*, 41, 257–275.

Lanteri, A. (2018): "The Market for Used Capital: Endegenous Irreversibility and Reallocation over the Business Cycle," *American Economic Review*, 108(9), 2383–2419.

Leduc, S., and Z. Liu (2016): "Uncertainty Shocks are Aggregate Demand Shocks," *Journal of Monetary Economics*, 82, 20–35.

Ludvigson, S. C., S. Ma, and S. Ng (2019): "Uncertainty and Business Cycles: Exogenous Impulse or Endogenous Response?," *American Economic Journal: Macroeconomics*, forthcoming.

——— (2020): "COVID19 and The Macroeconomic Effects of Costly Disasters," available at https://www.sydneyludvigson.com/working-papers.

Pellegrino, G. (2017): "Uncertainty and Monetary Policy in the US: A Journey into Non-Linear Territory," available at https://sites.google.com/site/giovannipellegrinopg/home.

——— (2018): "Uncertainty and the Real Effects of Monetary Policy Shocks in the Euro Area," *Economics Letters*, 162, 177–181.

Pellegrino, G., F. Ravenna, and G. Züllig (2020): "The Impact of Pessimistic Expectations on the Effects of COVID-19-Induced Uncertainty in the Euro Area," available at https://sites.google.com/site/giovannipellegrinopg/home.

Piffer, M., and M. Podstawski (2018): "Identifying uncertainty shocks using the price of gold," *Economic Journal*, 128(616), 3266–3284.

Rotemberg, J. J. (1982): "Monopolistic Price Adjustment and Aggregate Output," *Review of Economic Studies*, 49, 517–531.

Rubio-Ramírez, J. F., D. F. Waggoner, and T. Zha (2010): "Structural Vector Autoregressions: Theory of Identification and Algorithms for Inference," *Review of Economic Studies*, 77, 665–696.

Rudebusch, G. D., and E. T. Swanson (2012): "The Bond Premium in a DSGE Model with Long-Run Real and Nominal Risks," *American Economic Journal: Macroeconomics*, 4(1), 105–143.

Ruge-Murcia, F. (2014): "Indirect Inference Estimation of Nonlinear Dynamic General Equilibrium Models: With an Application to Asset Pricing under Skewness Risk," CIREQ, Cahiers de Recherche No. 15-2014.

Schildberg-Horisch, H. (2018): "Are Risk Preferences Stable?," *Journal of Economic Perspectives*, 32, 135–154.

Schmitt-Grohe, S., and M. Uribe (2004): "Solving Dynamic General Equilibrium Models Using a Second-Order Approximation to the Policy Function," *Journal of Economic Dynamics and Control*, 28, 755–775.

Sims, E., and C. Wu (2020): "Evaluating Central Banks' Tool Kit: Past, Present, and Future," *Journal of Monetary Economics*, forthcoming.

Stock, J. H., and M. W. Watson (2012): "Disentangling the Channels of the 2007-2009 Recession," *Brookings Papers on Economic Activity*, Spring, 81–135.

Swanson, E. T. (2012): "Risk Aversion and the Labor Margin in Dynamic Equilibium Models," *American Economic Review*, 102, 1663–1691.

——— (2018): "Risk Aversion, Risk Premia, and the Labor Margin with Generalized Recursive Preferences," *Review of Economic Dynamics*, 28, 290–321.

Teräsvirta, T. (2018): "Nonlinear Models in Macroeconometrics," Oxford Research Encyclopedias in Economics and Finance, Oxford: Oxford University Press.

Teräsvirta, T., D. Tjøstheim, and C. W. Granger (2010): "Modeling Nonlinear Economic Time Series," Oxford University Press, Oxford.

Wu, J. C., and F. D. Xia (2016): "Measuring the Macroeconomic Impact of Monetary Policy at the Zero Lower Bound," *Journal of Money, Credit, and Banking*, 48(2-3), 253–291.

Event constraints			
t	Event	Source	Constraint on $e_{FU.t}$
1962Q4	Cuban missile crisis	B	$e_{FU.t} \geqslant p(\mathbf{e}_{FUt}(\boldsymbol{B}), 50th)$
1963Q4	Assassination of JFK	B	$e_{FU.t} \geqslant p(\mathbf{e}_{FUt}(\boldsymbol{B}), 50th)$
1966Q3	Vietnam buildup	B	$e_{FU.t} \geqslant p(\mathbf{e}_{FUt}(\boldsymbol{B}), 50th)$
1970Q2	Cambodia and Kent state	B	$e_{FU.t} \geqslant p(\mathbf{e}_{FUt}(\boldsymbol{B}), 50th)$
1973Q4	OPEC I, Arab-Israeli War	B	$e_{FU.t} \geqslant p(\mathbf{e}_{FUt}(\boldsymbol{B}), 50th)$
1974Q3	Franklin National	B	$e_{FU.t} \geqslant p(\mathbf{e}_{FUt}(\boldsymbol{B}), 50th)$
1978Q4	OPEC II	B	$e_{FU.t} \geqslant p(\mathbf{e}_{FUt}(\boldsymbol{B}), 50th)$
1979Q4	Volcker experiment	B, LMN	$e_{FU.t} \geqslant p(\mathbf{e}_{FUt}(\boldsymbol{B}), 50th)$
1980Q1	Afghanistan, Iran hostages	B	$e_{FU.t} \geqslant p(\mathbf{e}_{FUt}(\boldsymbol{B}), 50th)$
1982Q4	Monetary policy turning point	B	$e_{FU.t} \geqslant p(\mathbf{e}_{FUt}(\boldsymbol{B}), 50th)$
1987Q4	Black Monday	B, LMN	$e_{FU.t} \geqslant p(\mathbf{e}_{FUt}(\boldsymbol{B}), 75th)$
1990Q4	Gulf War I	B	$e_{FU.t} \geqslant p(\mathbf{e}_{FUt}(\boldsymbol{B}), 50th)$
1991Q4	Dissolution of the Soviet Union	B	$e_{FU.t} \geqslant p(\mathbf{e}_{FUt}(\boldsymbol{B}), 50th)$
1997Q4	Asian crisis	B	$e_{FU.t} \geqslant p(\mathbf{e}_{FUt}(\boldsymbol{B}), 50th)$
1998Q3	Russian, LTCM default	B	$e_{FU.t} \geqslant p(\mathbf{e}_{FUt}(\boldsymbol{B}), 50th)$
2001Q3	9/11	B	$e_{FU.t} \geqslant p(\mathbf{e}_{FUt}(\boldsymbol{B}), 50th)$
2002Q3	Worlcom, Enron	B	$e_{FU.t} \geqslant p(\mathbf{e}_{FUt}(\boldsymbol{B}), 50th)$
2003Q1	Iraq invasion	B	$e_{FU.t} \geqslant p(\mathbf{e}_{FUt}(\boldsymbol{B}), 50th)$
2008Q4	Great recession	B, LMN	$e_{FU.t} \geqslant p(\mathbf{e}_{FUt}(\boldsymbol{B}), 75th)$
2011Q3	Debt ceiling crisis	LMN	$e_{FU.t} \geqslant p(\mathbf{e}_{FUt}(\boldsymbol{B}), 50th)$
2016Q1	End of the US ZLB in the US, China, Japanese neg. rate, Brexit refer. ann.	This paper	$e_{FU.t} \geqslant p(\mathbf{e}_{FUt}(\boldsymbol{B}), 50th)$

External variable constraints		
External variable S_t	Source	Constraint on $\rho(e_{FUt}, S_t)$
Stock market return	LMN	$\rho(e_{FUt}, S_t) \leqslant p(\rho(e_{FUt}, S_t), 50th)$
Real price of gold (log difference)	LMN	$\rho(e_{FUt}, S_t) \geqslant p(\rho(e_{FUt}, S_t), 50th)$

Table 1: **Event and external variable constraints.** Constraints imposed to identify financial uncertainty shocks. Sources: B = Bloom (2009); LMN = Ludvigson et al. (2019). p(X,Zth) refers to the Zth percentile of the empirical density of the variable X.

	Output	Consumpt.	Investment	Hours
Baseline IVAR and VAR				
Peak response: Linear	-1.54%	-1.03%	-3.34%	-1.90%
Peak response: Great Recession	-2.32%	-1.36%	-8.32%	-3.75%
Ratio GR/Linear	1.50	1.32	2.49	1.97

Table 2: **Peak responses.** Peak responses to a one standard deviation uncertainty shock estimated with linear VAR and nonlinear IVAR for the great recession.

		Priors	Posteriors	
			Linear VAR	Great Recession
Parameter	Interpretation	D(mean, std)	Mode, std	Mode, std
ρ_{σ^a}	Unc. shock, persistence	B(0.77, 0.10)	**0.64,** 0.03	**0.65,** 0.03
b	Habit formation parameter	B(0.75, 0.15)	**0.64,** 0.06	**0.66,** 0.04
ϕ_K	Investment adjustment costs	G(3.92, 2)	**2.29,** 0.50	**3.21,** 0.60
ϕ_P	Price adjustment costs	G(240, 40)	**236.78,** 32.26	**282.10,** 33.54
ρ_π	Taylor rule parameter, inflation	IG(1.5, 0.25)	**1.05,** 0.01	**1.05,** 0.01
ρ_y	Taylor rule parameter, output growth	G(0.2, 0.15)	**0.20,** 0.04	**0.28,** 0.05
σ	Risk aversion (fixed labor supply, no habits)	G(100, 60)	**385.90,** 50.45	**533.04,** 59.16
RRA	Risk aversion (endogenous labor supply, habits)		**104.85**	**144.96**

Table 3: **DSGE model: Average evidence vs. Great recession.** Values estimated conditional on both the linear VAR impulse responses and on the IVAR impulse responses in 2008Q4. Standard deviations estimated conditional on a Laplace approximation of the posterior density. Risk aversion in the model (RRA) computed by considering endogenous labor supply and habits as in Swanson (2018).

	Output	Consumpt.	Investment	Hours
Peak responses				
Covid-19 Optimistic	-2.47%	-1.39%	-5.88%	-1.67%
Covid-19 Intermediate	-4.47%	-2.55%	-10.62%	-3.03%
Covid-19 Pessimistic	-6.50%	-3.70%	-15.47%	-4.39%
Great Recession	-2.47%	-1.39%	-5.88%	-1.67%
Cumulative responses				
Covid-19 Optimistic	-35.20%	-19.30%	-81.90%	-22.60%
Covid-19 Intermediate	-63.90%	-35.63%	-147.48%	-41.00%
Covid-19 Pessimistic	-92.64%	-51.92%	-213.05%	-59.36%
Great Recession	-35.20%	-19.30%	-81.90%	-22.60%

Table 4: **Covid19.** Peak and cumulative responses for the great recession and Covid-19 based on the estimated DSGE model

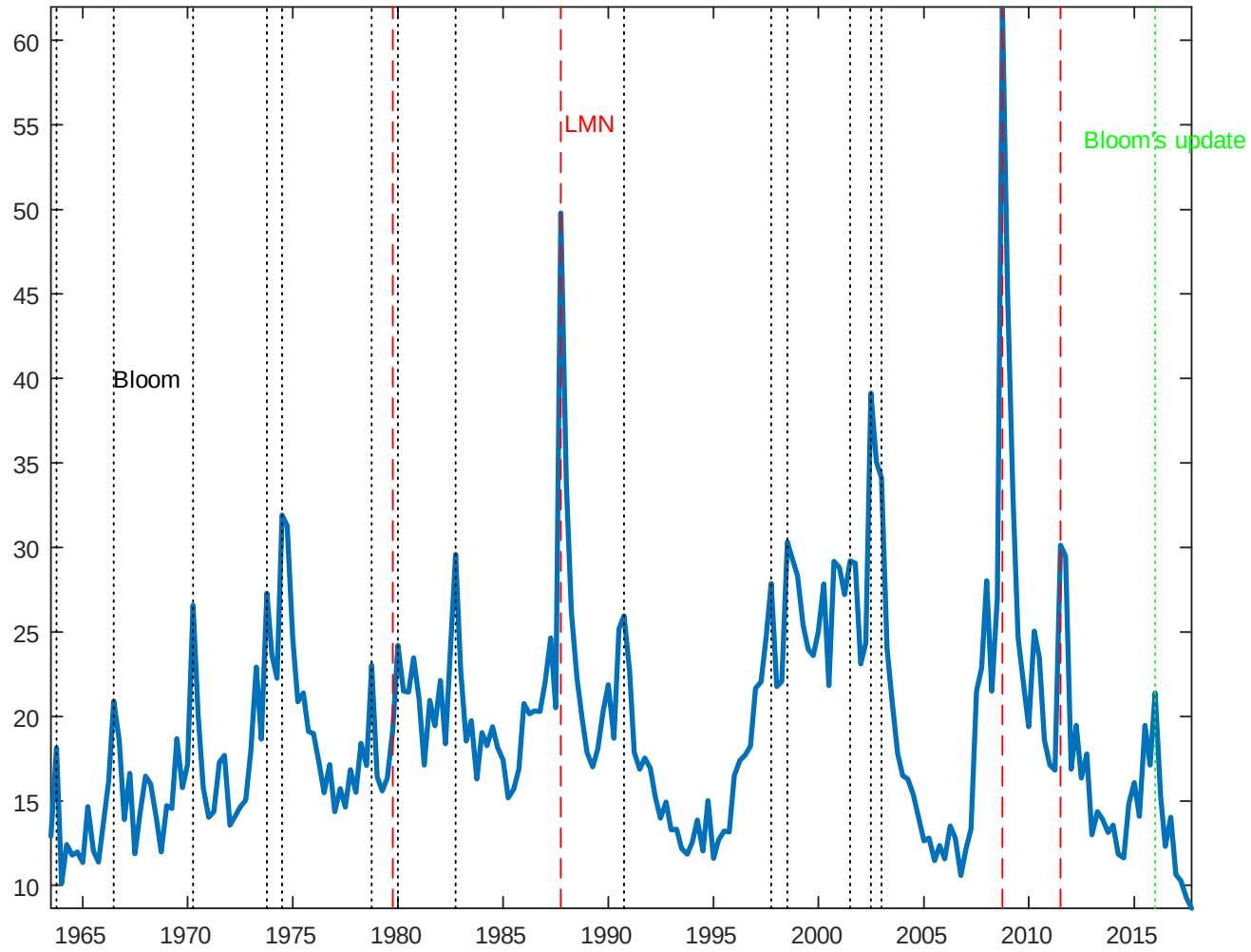

Figure 1: **Financial uncertainty: Identified peaks.** Vertical lines identify the events used to identify financial uncertainty shocks. The four red lines refer to the events selected by Ludvigson, Ma and Ng (2019). The black lines identify the dates selected by Bloom (2009). The green line refers to the 2016 increase not covered in Bloom (2009). Further details are reported in Table 1.

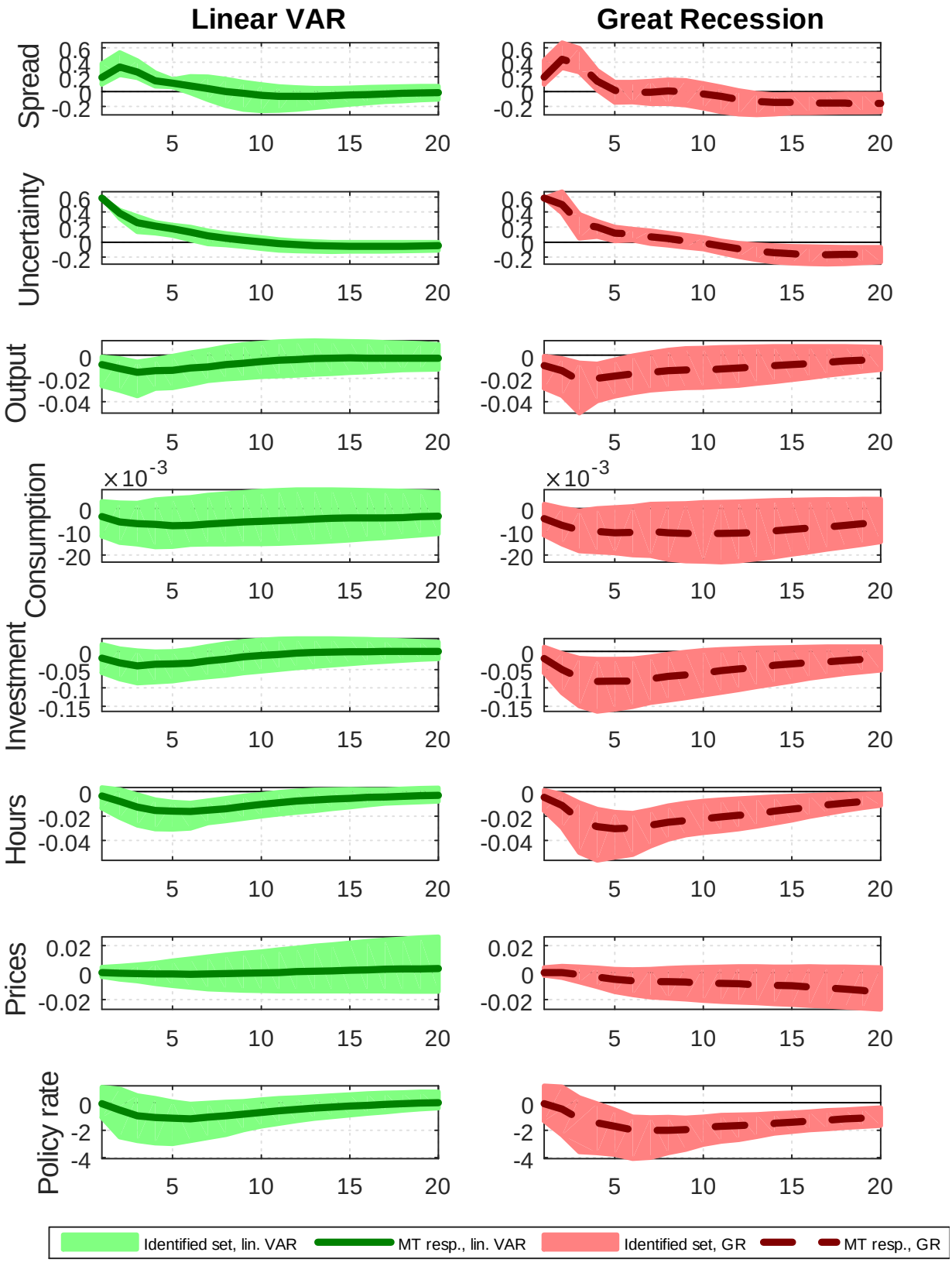

Figure 2: **Impulse responses: linear vs. great recession.** Impulse responses to a 4.4-standard deviation uncertainty shock. The solid green (red) areas report the identified set of responses produced with the linear (nonlinear) VAR models. The solid (dashed) lines report the median target impulse response for the linear (nonlinear) VAR. The number of retained draws, out a total of one million draws, is 2,168 for the IVAR and 2,116 for the linear VAR.

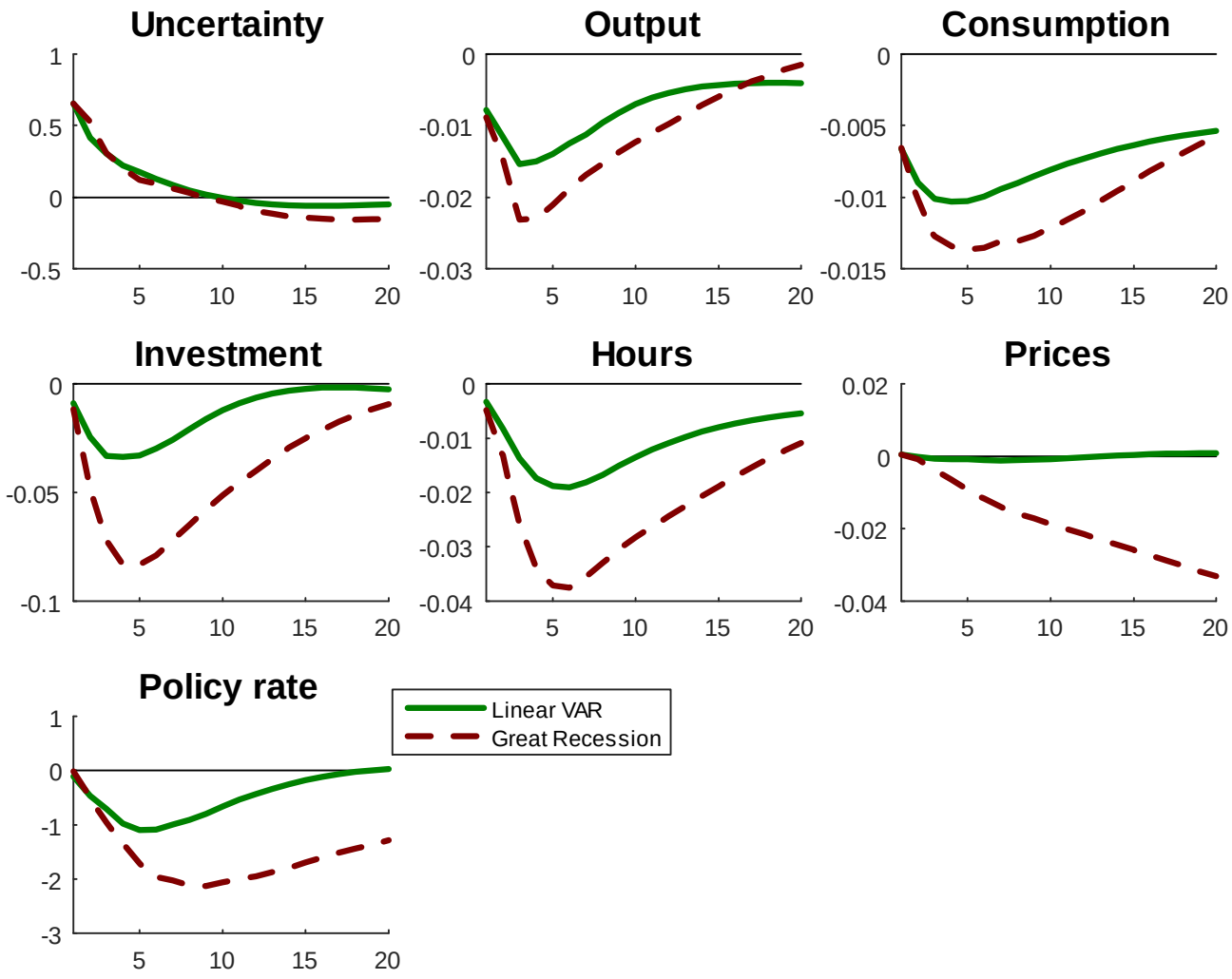

Figure 3: **Impulse responses: Fry and Pagan's (2011) median target IRFs.** The solid green line reports the median target (MT) impulse response for the linear VAR. The dashed red line is the MT impulse response obtained from the IVAR for the great recession.

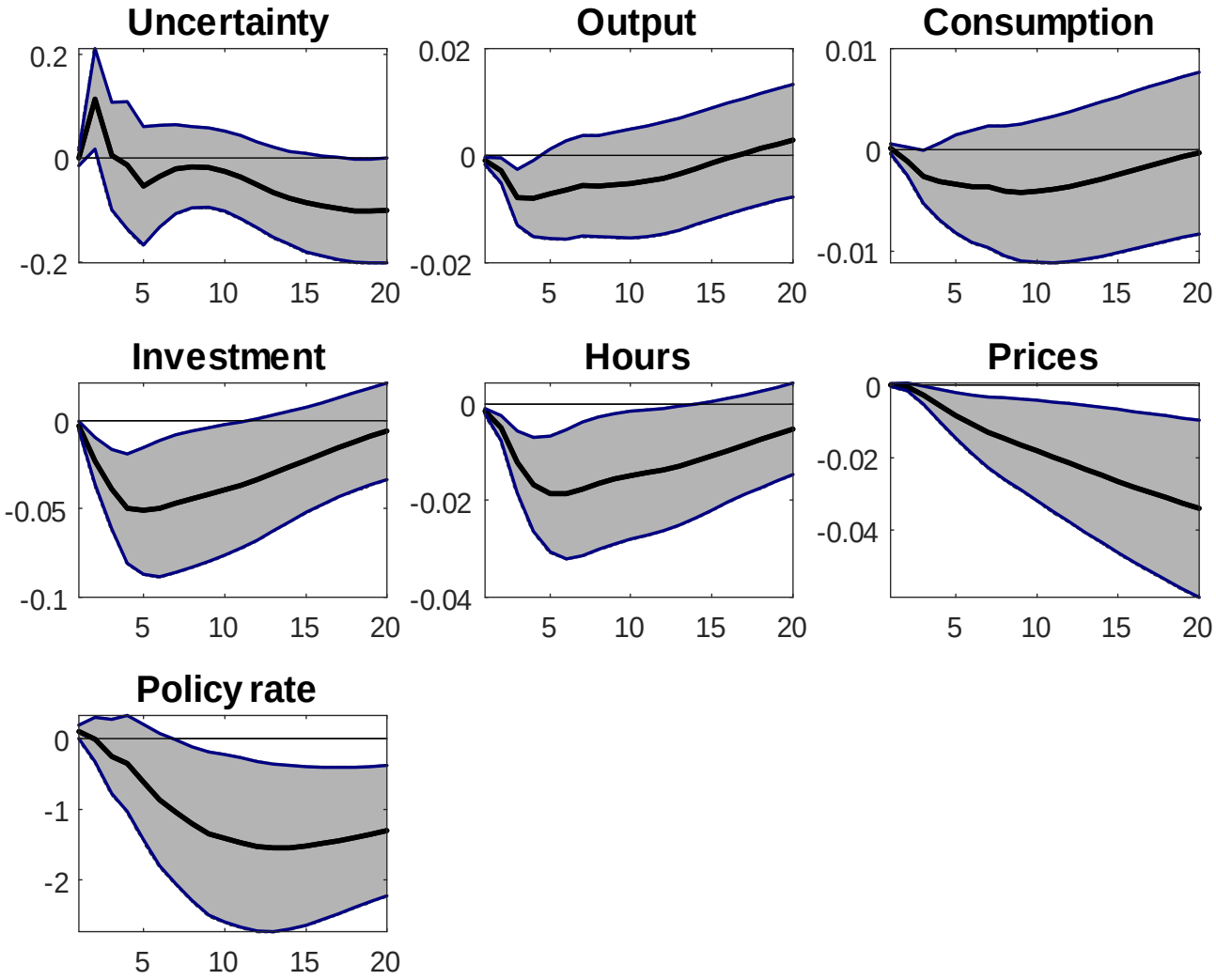

Figure 4: **Bootstrapped test for the difference of median target responses.** Grey bands: 90% confidence bands.

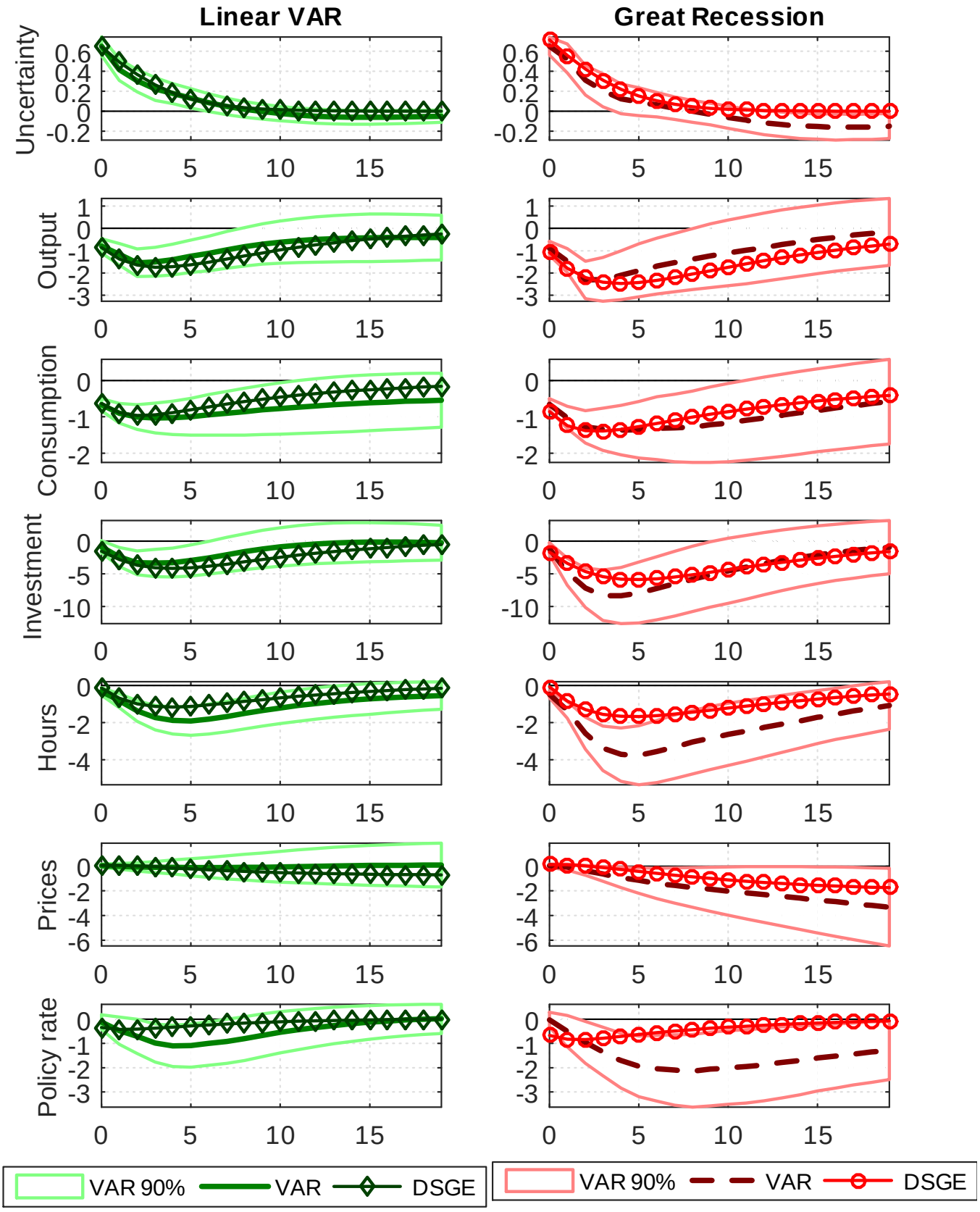

Figure 5: **VAR and DSGE impulses responses to an uncertainty shock: Linear VAR vs. nonlinear VAR (great recession).** Solid green line: linear VAR impulse responses with 90% confidence bands. Solid black lines with squares: Responses of the DSGE model estimated with linear VAR moments. Dashed red lines: IVAR impulse reponses for the great recession with 90% confidence bands. Solid red lines with circles: Responses of the DSGE model estimated with nonlinear VAR moments. VAR estimated with four lags.

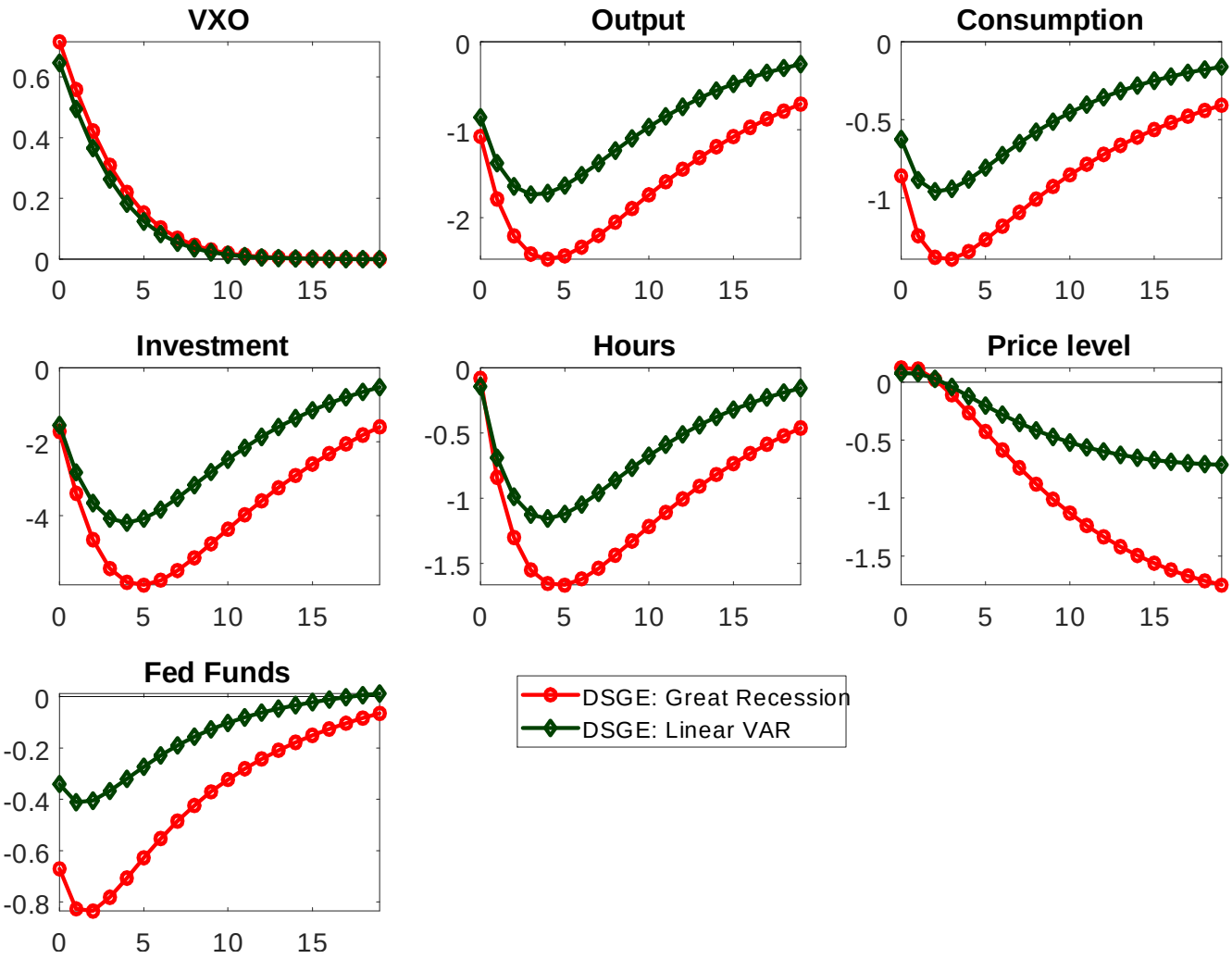

Figure 6: **DSGE impulses responses: Linear vs. great recession.** Responses computed by calibrating the DSGE framework with the posterior modes of the estimated structural parameters.

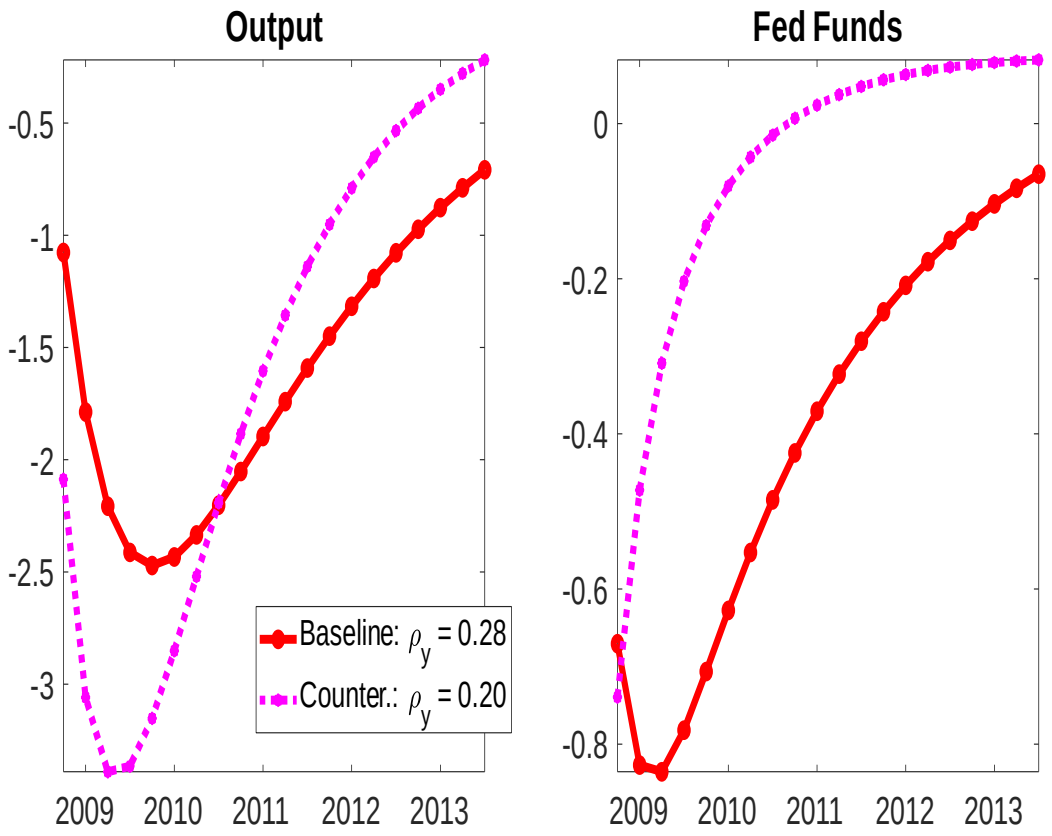

Figure 7: **Counterfactual experiment on the role of monetary policy for the propagation of the 2008Q4 uncertainty shocks and the depth of the great recession.** Baseline: GIRFs conditional on the parameters estimated with the great recession impulse responses. Counterfactual experiment conducted by replacing the Taylor rule parameter $\rho_y^{GR} = 0.28$ with the "normal times" value $\rho_y^{linear} = 0.20$.

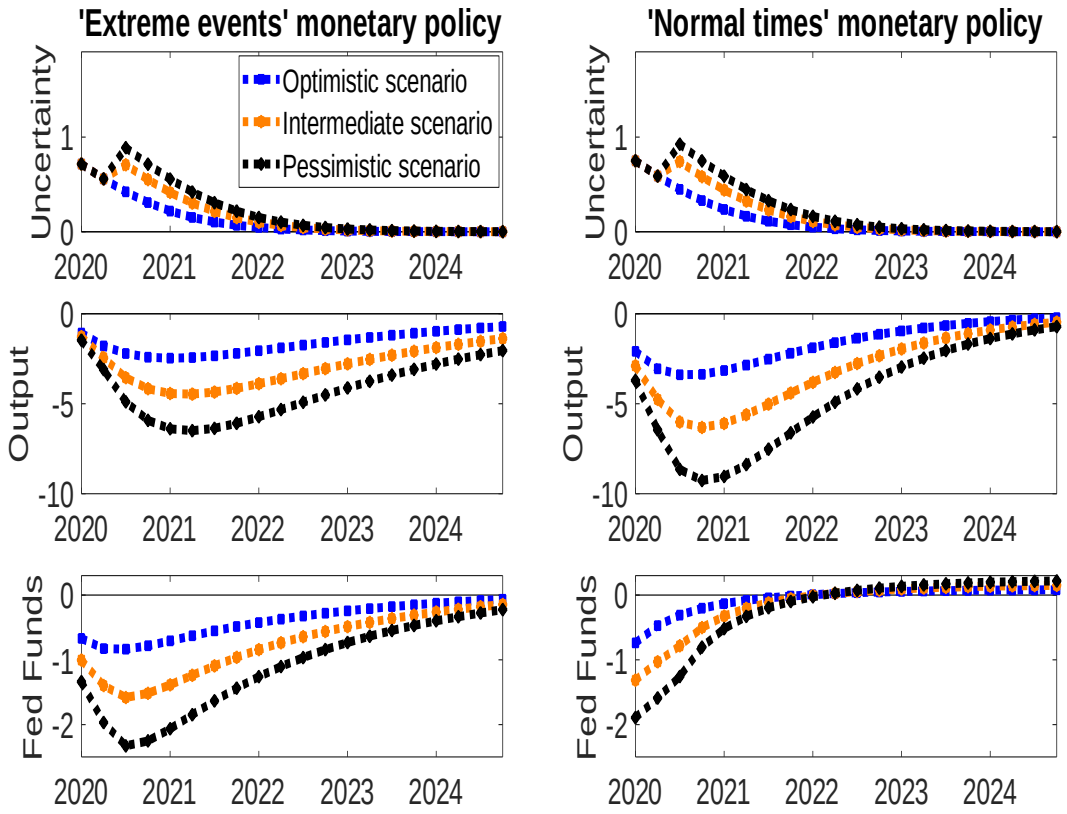

Figure 8: **Counterfactual experiment on the role of monetary policy for the propagation of the Covid-19-induced uncertainty shock.** "Optimistic scenario": Uncertainty shock in 2020Q1 only. "Intermediate scenario": Uncertainty shock in 2020Q1 plus moderate uncertainty shock in 2020Q3. "Pessimistic scenario": Uncertainty shock in 2020Q1 plus large uncertainty shock in 2020Q3.

Appendix of the paper "Uncertainty and Monetary Policy During Extreme Events", by Giovanni Pellegrino, Efrem Castelnuovo, and Giovanni Caggiano

This Appendix contains additional material with respect to the contents of our paper. In particular:

- Section A offers details on the way we compute the generalized impulse responses (GIRFs) with our nonlinear VAR;
- Section B documents additional results obtained with our nonlinear VAR analysis. In particular, our results are robust to: a) adding extra interaction terms to our baseline nonlinear VAR framework; b) accounting for model uncertainty; c) controlling for a proxy of credit spread, which is meant to capture first-moment financial shocks;
- Section C shows that our event-based approach for the identification of uncertainty shocks works well if the data generating process is the Basu and Bundick (2017) model;
- Section D derives the formula we use in the paper to compute the value of the relative risk aversion in the estimated DSGE framework, which depends (as also explained in the text of the paper) on the structure of the economy because of the presence of habits in consumption and endogenous labor supply;
- Section E offers details on the Bayesian IRFs matching econometric strategy used in the paper to estimate the DSGE framework in a state-dependent fashion;
- Section F discusses the calibration of the set of structural parameters of the DSGE model we work which we do not estimate;
- Section G documents the counterfactual simulations conducted to identify the crucial parameters behind the different dynamic responses of the endogenous variables modeled with the DSGE framework to an uncertainty shock;
- Section H shows that initial conditions do not materially affect the generalized impulse responses computed with our DSGE framework.

A: Computation of the Generalized Impulse Response Functions

The algorithm for the computation of the Generalized Impulse Response Functions follows the steps suggested by Koop, Pesaran, and Potter (1996), and it is designed to simulate the effects of an orthogonal structural shock as in Kilian and Vigfusson (2011). The idea is to compute the empirical counterpart of the theoretical $GIRF_{\mathbf{Y}}(h, \delta, \boldsymbol{\omega}_{t-1})$ of the vector of endogenous variables $\mathbf{y}_t$, h periods ahead, for a given initial condition $\boldsymbol{\omega}_{t-1} = \{\mathbf{Y}_{t-1}, ..., \mathbf{Y}_{t-k}\}$, where k is the number of VAR lags, and δ is the structural shock hitting at time t. Following Koop, Pesaran, and Potter (1996), such GIRF can be expressed as follows:

$$GIRF_{\mathbf{Y}}(h, \delta, \boldsymbol{\omega}_{t-1}) = E[\mathbf{Y}_{t+h} \,|\delta, \boldsymbol{\omega}_{t-1}] - E[\mathbf{Y}_{t+h} \,|\boldsymbol{\omega}_{t-1}]$$

where $E[\cdot]$ is the expectation operator, and $h = 0, 1, ..., H$ indicates the horizons from 0 to H for which the computation of the GIRF is performed.

In our case, $\boldsymbol{\omega}_{t-1}$ corresponds to our "Great Recession" initial condition, i.e., the initial condition corresponding to the uncertainty spike occurred in $t = 2008Q4$ or:

$$\boldsymbol{\omega}_{t-1} = \boldsymbol{\omega}_{2008Q3} = \{\mathbf{Y}_{2008Q3}, ..., \mathbf{Y}_{2008Q3-k+1}\}.$$

Notice that, given that uncertainty and GDP are modeled in the VAR, such set includes the values of the interaction terms $(\ln VXO \times \Delta \ln GDP)_{t-j}$, $j = 1, ..., k$.

Given our IVAR model (formalized in the paper, see eq. (1)), we compute our GIRFs as follows:

1. use the initial condition $\boldsymbol{\omega}_{t-1} = \boldsymbol{\omega}_{2008Q3}$. Pick a matrix $\mathbf{B}$ among the set of retained matrices $\overline{\mathcal{B}}$ that satisfy our identifying narrative sign restrictions (see identification in Section 2 of the paper);

2. conditional on $\boldsymbol{\omega}_{t-1}$, $\mathbf{B}$ and the structure of the model (1), we simulate the path $[\mathbf{Y}_{t+h} \,|\boldsymbol{\omega}_{t-1}]^r$, $h = [0, 1, ..., 19]$ (which is, realizations up to 20-step ahead) by loading our VAR with a sequence of randomly extracted (with repetition) residuals $\widetilde{\boldsymbol{\eta}}^r_{t+h} \sim d(0, \boldsymbol{\Omega})$, $h = 0, 1, ..., H$, where $\boldsymbol{\Omega}$ is the VCV matrix of the IVAR residuals, $d(\cdot)$ is the empirical distribution of the residuals, and r indicates the particular sequence of residuals extracted;

3. conditional on $\boldsymbol{\omega}_{t-1}$, $\mathbf{B}$ and the structure of the model (1), we simulate the path $[\mathbf{Y}_{t+h} \,|\delta, \boldsymbol{\omega}_{t-1}]^r$, $h = [0, 1, ..., 19]$ by loading our VAR with a perturbation of the

randomly extracted residuals $\widetilde{\mathbf{u}}_{t+h}^{r} \sim d(0, \boldsymbol{\Omega})$ obtained in step 2. In particular, we use the decomposition $\boldsymbol{\Omega} = \boldsymbol{B}\boldsymbol{B}'$, where $\boldsymbol{B}$ is the picked admissible solution. Hence, we recover the orthogonalized elements (shocks) $\widetilde{\mathbf{e}}_{t}^{r} = \boldsymbol{B}^{-1}\widetilde{\boldsymbol{\eta}}_{t}^{r}$. We then add a quantity $\delta > 0$ to the $\widetilde{e^{r}}_{unc,t}$, where $\widetilde{e^{r}}_{unc,t}$ is the scalar stochastic element loading the uncertainty equation in the VAR. This enable us to obtain $\widetilde{\mathbf{e}}_{t}^{r}$, which is the vector of perturbed orthogonalized elements embedding $\widetilde{e^{r}}_{unc,t}$. We then move from perturbed shocks to perturbed residuals as follows: $\widetilde{\boldsymbol{\eta}}_{t}^{r} = \boldsymbol{B}\widetilde{\mathbf{e}}_{t}^{r}$. These are the perturbed residuals that we use to simulate $[\mathbf{Y}_{t+h} \,|\delta, \boldsymbol{\omega}_{t-1}]^{r}$;

4. we compute the difference between paths for each simulated variable at each simulated horizon $[\mathbf{Y}_{t+h} \,|\delta, \boldsymbol{\omega}_{t-1}]^{r} - [\mathbf{Y}_{t+h} \,|\boldsymbol{\omega}_{t-1}]^{r}$, $h = [0, 1, ..., 19]$;

5. we repeat steps 2-4 a number of times equal to $R = 500$. We then store the horizon-wise average realization across repetitions r. In doing so, we obtain a consistent estimate of the GIRF given the matrix $\mathbf{B}$, $\widehat{GIRF}^{\mathbf{B}}_{\mathbf{Y}}(h, \delta_t, \boldsymbol{\omega}_{t-1}) = \widehat{E}[\mathbf{Y}_{t+h} \,|\delta, \boldsymbol{\omega}_{t-1}] - \widehat{E}[\mathbf{Y}_{t+h} \,|\boldsymbol{\omega}_{t-1}]$, $h = [0, 1, ..., 19]$;

6. we repeat steps 1-5 for each given matrix $\boldsymbol{B}$ among the set of retained matrices $\overline{\mathcal{B}}$. The set of all the GIRFs for each possible $\mathbf{B} \in \mathcal{B}$ determines our identified set. If a given matrix $\mathbf{B}$ leads to an explosive response (namely if this is explosive for most of the R sequences of residuals $\widetilde{\boldsymbol{\eta}}_{t+h}^{r}$, in the sense that the response of the shocked variable diverges instead than reverting to zero), then such initial condition is discarded.[1] In order to plot a summary GIRF out of this set we use the Median Target (MT) response proposed by Fry and Pagan (2011), i.e., the GIRF corresponding to the $\mathbf{B}$ model whose implied impulse responses to an uncertainty shock are the closest to the median responses computed across all retained models;

7. confidence bands surrounding the MT GIRFs estimates obtained in step 6 are computed via a bootstrap procedure. In particular, we simulate $S = 1,000$ samples of size equivalent to the one of actual data. Then, per each simulated dataset, we: i) estimate our nonlinear VAR model; ii) implement step 5.[2] In implementing

[1] This never happens for our responses estimated on actual data. We verified that it happens quite rarely as regards our bootstrapped responses.

[2] Per each simulated set we also estimate the linear VAR specification nested in the IVAR model and compute the corresponding linear response to the same shock size, so that to be consistent with what we do on the actual data. The bootstrap used is similar to the one used by Christiano, Eichenbaum, and Evans (1999) (see their footnote 23). The code discards the explosive artificial draws to be sure that exactly 1,000 draws are used. In our simulations, this happens a negligible fraction of times.

this procedure the initial conditions and VCV matrix used for our computations now depend on the particular dataset s used, i.e., $\boldsymbol{\omega}_{t-1}^s$ and $\boldsymbol{\Omega}_t^s$.[3] Hence, rather than using the $\mathbf{B}$ which corresponds to the MT response, we use the rotation $\mathbf{Q}$ which corresponds to the MT response, i.e., we use $\mathbf{B}^s = P^s\mathbf{Q}$ with P^s being the unique lower-triangular Cholesky factor associated to $\boldsymbol{\Omega}_t^s$, i.e., $\boldsymbol{\Omega}_t^s = P^s P^{s\prime}$. Confidence bands are constructed by considering the point estimates of the impulse responses ± 1.64 times the bootstrapped standard errors.

We use a shock size δ equal to the median size of the uncertainty shock in $t = 2008Q4$ among all retained shocks series.

B: Extra results on the IVAR analysis

Parsimonious (baseline) vs. extended IVAR

The IVAR model employed in the paper is a parsimonious version of a more sophisticated IVAR which we estimated to check the robustness of our results. Thinking of the third-order approximation of the DSGE model we work with, it is natural to extend our baseline IVAR framework to add extra interaction terms involving quadratic terms as follows:

$$\mathbf{Y}_t = \boldsymbol{\alpha} + \sum_{j=1}^{L} \mathbf{A}_j \mathbf{Y}_{t-j} + \begin{bmatrix} \sum_{j=1}^{L} \mathbf{c}_j \ln VXO_{t-j} \times \Delta \ln GDP_{t-j} \\ + \sum_{j=1}^{L} \mathbf{c}_j (\ln VXO_{t-j})^2 \times \Delta \ln GDP_{t-j} \\ + \sum_{j=1}^{L} \mathbf{c}_j \ln VXO_{t-j} \times (\Delta \ln GDP_{t-j})^2 \end{bmatrix} + \mathbf{u}_t$$

Cubic terms $((\ln VXO_{t-j})^3, (\Delta \ln GDP_{t-j})^3)$ are omitted to minimize the likelihood of explosiveness.

Figure A1 contrasts the impulse responses obtained with our baseline model with those produced with the enriched framework. If anything, the reactions produced by this framework speak even more clearly in favor of nonlinearities in the data.

Model uncertainty

Figure 4 in the main text shows the outcome of a test for the difference of median target responses that only accounts for estimation (or sampling) uncertainty by means of the bootstrap at point 7. Figure A2 instead shows a test for the difference of state-dependent responses that focuses on model uncertainty, i.e., on the uncertainty related to all the

[3] To maximize comparability between the initial condition $\boldsymbol{\omega}_{t-1}^s$ and the Great Recession one in the actual sample, in the simulated dataset we pick the quarter t with the biggest uncertainty spike.

responses in the identified set. The differences are constructed as follows. We start by considering the same set of rotations for both the linear and the interacted VARs. Among all retained draws for each model, we consider only those that are common to the two VARs. This leaves us with 77% of common retained draws. We then construct the difference among the responses belonging to the set of common retained draws and plot their distribution. Figure A2 shows that all differences remain significant, even when looking at the 90% percentile of the empirical distribution.

A test accounting both for estimation and for model uncertainty is not proposed here. Such a test would be extremely demanding from a computational standpoint, given that our VAR model is a nonlinear one and the computation of the GIRFs is time-consuming. A test of this sort is proposed by Ludvigson, Ma, and Ng (2019), who - however - focus on a linear framework and, therefore, can compute impulse responses pretty quickly given that such responses are independent from initial conditions and do not require averaging out the outcome of different simulations accounting for different initial conditions.

The role of first moment shocks

The Basu and Bundick (2017) model features frictionless financial markets. As such, it acknowledges no role to first moment financial shocks as drivers of the business cycle. Consistently with Basu and Bundick's (2017) theoretical framework, our baseline VAR specification(s) does not feature any measure of financial frictions. However, as discussed by Stock and Watson (2012), the great recessions was likely caused by a combination of first-moment financial shocks and uncertainty shocks. Hence, one may wonder if our finding on the larger business cycle effects caused by uncertainty shocks during the great recession is in fact an artifact due to having left out of the picture the role of first moment financial shocks. To address this issue, we augment our baseline vector in the IVAR specification with a measure of spread, which is meant to capture frictions in financial markets. Our model of endogenous variables is then given by: $\mathbf{Y}_t = [SPREAD, \ln VXO, \ln GDP, \ln C, \ln I, \ln H, \ln P, FFR]'$, where $SPREAD$ is the difference between the BAA yield and the AAA one, VXO denotes the stock market S&P 100 implied volatility index, GDP per capita GDP, C per capita consumption, I per capita investment, H per capita hours worked, P the price level, and FFR the federal funds rate. To jointly identify first and second moment (uncertainty) financial shocks we adopt the same methodology of Section 2. The narrative sign restrictions approach has the clear advantage of not imposing any timing restrictions on

the spread-uncertainty contemporaneous relationship. This implies that, conditional on our identification strategy to separate first and second-moment financial shocks, the results we obtain are not driven by questionable zero restrictions.

The challenge at this point is to disentangle spread and uncertainty shocks, which are typically assumed to have similar effects on macro variables. To separate the two shocks, we impose the following restrictions. First, our uncertainty shock in 1987Q4 (the quarter related to the Black Monday) has to be greater than or equal to the 75th percentile of the distribution of the shocks conditional on that quarter. In other words, the uncertainty shock must be "sufficiently large". Differently, our first moment financial shock in 1987Q4 has to be smaller than or equal to the median. This second requirement is supported by the evidence provided by Gilchrist and Zakrajšek (2012), whose measure of financial frictions - the excess bond premium calculated as the fraction of a microfounded credit spread index not explained by the underlying fundamentals of bond issuers - has a negative spike in October 1987. Figure A3 plots our proxy of uncertainty, the VXO, along with three commonly used measures of financial frictions: the Baa-Aaa spread, the excess bond premium estimated by Gilchrist and Zakrajšek (2012), and the National Financial Conditions Index produced by the Chicago Fed. While all indicators show a large spike in the great recession, in October 1987 only the VXO experienced a large increase, while all other indicators displayed value below their average.

The second event-based identifying restriction we impose to separate first and second-moment financial shocks is that our first-moment financial shock in 2008Q4 be greater than or equal to the median shock. This requirement is similar to that imposed for the identification of our financial uncertainty shock. The 2008Q4-related restriction is meant to make sure that we just retain models pointing to large financial shocks (both first and second-moment financial shocks) during the great recession.

Figure A4 reports the set identified GIRFs to an uncertainty shock for the great recession scenario based on the IVAR model, as well as the impulse responses for the linear case. Figure A5 reports the Median Target (G)IRFs and Figure A6 the difference between the linear and the nonlinear case, along with one and two standard deviations confidence bands. Two results stand out. First, the recessionary impact on all real activity indicators is larger, and statistically significant, in the great recession. Second, the peak responses are virtually the same compared with the baseline scenario (documented in Figures 2 and 3 in the paper). Hence, our results are robust to controlling for a measure of financial frictions in our VAR. Finally, Table A1 documents the similarity

between some moments implied by our baseline IVAR and the same moments produced with the IVAR enriched with financial frictions presented in this Section.

C: Narrative Sign Restrictions and DSGE framework

This Section shows that the narrative sign restrictions (NSR) approach proposed in the paper is able to recover the true impulse responses to an uncertainty shock conditional on the Basu and Bundick (2017) model being the data generating process.

The Basu and Bundick (2017) model features an endogenous measure of financial uncertainty, a model-consistent VXO, which responds to three shocks, i.e., a first-moment technology shock, a first-moment preference shock, and a second-moment preference shock, this last one being the uncertainty shock. The question is whether it is possible to identify uncertainty shocks only by observing the VXO, as we do in the data. To address this question, we simulate a sample of 2,500 observations with the Basu and Bundick (2017) model conditional on the estimates we obtained with the facts established by the linear VAR.[4] We then estimate a linear VAR and produce impulse responses to an uncertainty shock identified via our NSR restrictions.[5] In particular, consistently with what Bloom (2009) does to identify the dates we use in our baseline analysis, we select the dates with the biggest spikes in the HP-filtered (model-consistent) VXO.[6] Similarly to our baseline analysis, we require the realizations of our identified uncertainty shocks to be larger than the median value of the empirical density of the uncertainty shocks in the selected dates.[7] We focus on a population analysis and on a linear VAR to make sure that our result is not driven by any small-sample issue or fancy nonlinear reduced-form framework.

Figure A7 documents the performance of the NSR-VAR in replicating the DSGE-model consistent impulse responses. The ability of the VAR to correctly capture the

[4] Even if we employ a DSGE model with three shocks to simulate data which we use to estimate a seven variable-VAR model, no stochastic singularity issue arises in this exercise. The reason is that our data generating process is a nonlinear framework, hence perfect collinearity among the simulated series we use to estimate our VAR is not present even if the number of shocks is lower than the number of "observables" generated via those shocks.

[5] Although the word "narrative" loses its meaning for an exercise based on data simulated from a model, the proposed exercise resembles the identification strategy we use in our baseline analysis where uncertainty shocks are identified using information related to the VXO biggest spikes.

[6] We select the dates corresponding to the biggest 2% among VXO spikes. This selection seems appropriate because it guarantees that: i) enough responses are retained; ii) the selected dates are informative enough to identify the uncertainty shocks.

[7] Similarly to our baseline analysis and to Ludvigson, Ma, and Ng (2019), we impose that the correlation between the series of identified uncertainty shocks and (model-implied) stock market returns be smaller than the median value of the empirical density of the correlation coefficients for all draws.

responses of the DSGE model is unquestionable. This is good news not only for our VAR identification strategy, but also for the estimation of our DSGE framework. Indeed, the results in this Section imply that it makes sense to use a direct inference approach to estimate our DSGE framework, as opposed to a (much more computationally cumbersome) indirect inference approach, which would require the simulation of pseudo-data and the estimation of VAR impulse responses identified with NSR per each draw of the values of the structural parameters of the DSGE framework from its posterior density.

D: Relative Risk Aversion for the Basu and Bundick (2017) model extended with external habits

This Section derives the expression for the Relative Risk Aversion (RRA) coefficient in the version of the Basu and Bundick (2017) model extended with external habits and which features (as the original model) endogenous labor supply.

Equivalence with Rudebusch and Swanson's (2012) notation

It is first useful to clarify that the value function that we use, which is:

$$V_t = \left[\left(1-\beta \right) (a_t \tilde{C}_t^{\eta} (1-N_{t,})^{(1-\eta)} \right)^{(1-\sigma)/\theta_V} + \beta ((E_t V_{t+1})^{1-\sigma})^{1/\theta_V} \right]^{\theta_V/(1-\sigma)}$$

can be equivalently reformulated in Rudebusch and Swanson's (2012) notation as:

$$\tilde{V}_t = \tilde{U}_t(\tilde{C}_t, N_t) + \beta (E_t \tilde{V}_{t+1}^{(1-\alpha)})^{\frac{1}{(1-\alpha)}}.$$

where the $(1-\beta)$ pre-multiplying the contemporaneous utility function in the expression above is omitted for simplicity, given its irrelevance for the computation of the RRA. It can be easily shown that the two expressions are equivalent once the following definitions are used:

$$\begin{aligned} \tilde{V} &= V^{\frac{1-\sigma}{\theta_V}} \\ \alpha &= 1-\theta_V = 1 - \frac{1-\sigma}{1-\frac{1}{\psi}} \\ \tilde{U}_t(\tilde{C}_t, N_t) &= (a_t \tilde{C}_t^{\eta} (1-N_t)^{1-\eta})^{\frac{1-\sigma}{\theta_V}} \end{aligned}$$

Derivation of the formula for the RRA

Swanson (2012) shows that household's labor margin has substantial effects on risk aversion. The household can absorb asset return shocks either through changes in

consumption, changes in hours worked, or some combination of the two. This ability to absorb shocks along either or both margins greatly alters the household's attitudes toward risk. Following Swanson (2012) and Swanson (2018) (this latter paper extending the analysis in Swanson (2012) to - among other things - recursive preferences), we compute two measures of relative risk aversion for our model. The first measure - RRA^c - applies when there is no upper bound for labor and therefore total household wealth equals the present discounted value of consumption. The other measure - RRA^{cl} - applies when the upper bound for the household's time endowment is well-specified, meaning that total household wealth equals the present discounted value of leisure plus consumption.

Swanson (2018, equations 23 and 24) shows that, in presence of flexible labor margin and generalized recursive preferences, the expressions to compute the coefficient of steady state relative risk aversion read as follows:

$$\begin{aligned} RRA^{cl} &= \frac{-u_{11}+\lambda u_{12}}{u_1}\cdot\frac{C+w\left(1-N\right)}{1+w\lambda}+\alpha\frac{\left(C+w\left(1-N\right)\right)u_1}{u} \\ RRA^{c} &= \frac{-u_{11}+\lambda u_{12}}{u_1}\cdot\frac{C}{1+w\lambda}+\alpha\frac{Cu_1}{u} \end{aligned}$$

where:

$$\begin{aligned} w &= -\frac{u_2}{u_1} \\ \lambda &= \frac{wu_{11}+u_{12}}{u_{22}+wu_{12}} \end{aligned}$$

and where $u_1 = \frac{\partial \tilde{U}_t}{\partial C_t}\Big|_{ss}$, $u_2 = \frac{\partial \tilde{U}_t}{\partial N_t}\Big|_{ss}$, $u_{11} = \frac{\partial^2 \tilde{U}_t}{\partial C_t^2}\Big|_{ss}$, $u_{12} = \frac{\partial^2 \tilde{U}_t}{\partial C_t \partial N_t}\Big|_{ss}$, $u_{22} = \frac{\partial^2 \tilde{U}_t}{\partial N_t^2}\Big|_{ss}$, with ss standing for steady state, and where α and $\tilde{U}_t$ (or $\tilde{U}_t(\tilde{C}_t, N_t)$) were defined earlier. Variables without time subscript indicate steady state values.

It can be easily shown that (see Andreasen et al.'s (2018) Online Appendix):

$$RRA^{cl} = \left(1+\frac{w}{C}(1-N)\right)RRA^{c}.$$

Initial computations. Without loss of generality, the derivation below is based on the following function:[8]

$$\tilde{U}(C_t,N_t) = \frac{\left(\left(C_t-bC_{t-1}\right)^{\eta}\left(1-Nt\right)^{1-\eta}\right)^{\frac{1-\sigma}{\theta_V}}}{\frac{1-\sigma}{\theta_V}} = \frac{\left(C_t-bC_{t-1}\right)^{\eta\frac{1-\sigma}{\theta_V}}\left(1-N_t\right)^{(1-\eta)\frac{1-\sigma}{\theta_V}}}{\frac{1-\sigma}{\theta_V}}.$$

[8] We omit a_t from this derivation since its steady state value is 1, which implies that the impact of the preference shock on the relative risk aversion is zero.

We first take the relevant derivatives and then evaluate them at the steady state. Notice that the stock of external habits (bC_{t-1}) at time t is a given for households. Hence, we have:

$$\begin{aligned}
u_{1,t} &= \eta\left(C_t - bC_{t-1}\right)^{\eta\left(\frac{1-\sigma}{\theta_V}\right)-1}\left(1-N_t\right)^{(1-\eta)\left(\frac{1-\sigma}{\theta_V}\right)}, \\
u_{11,t} &= \eta\left(\eta\left(\frac{1-\sigma}{\theta_V}\right)-1\right)\left(C_t - bC_{t-1}\right)^{\eta\left(\frac{1-\sigma}{\theta_V}\right)-2}\left(1-N_t\right)^{(1-\eta)\left(\frac{1-\sigma}{\theta_V}\right)}, \\
u_{12,t} &= -\eta\left((1-\eta)\left(\frac{1-\sigma}{\theta_V}\right)\right)\left(C_t - bC_{t-1}\right)^{\eta\left(\frac{1-\sigma}{\theta_V}\right)-1}\left(1-N_t\right)^{(1-\eta)\left(\frac{1-\sigma}{\theta_V}\right)-1}, \\
u_{2,t} &= -\left(1-\eta\right)\left(C_t - bC_{t-1}\right)^{\eta\frac{1-\sigma}{\theta_V}}\left(1-N_t\right)^{(1-\eta)\frac{1-\sigma}{\theta_V}-1}, \\
u_{22,t} &= \left(1-\eta\right)\left(\left(1-\eta\right)\frac{1-\sigma}{\theta_V}-1\right)\left(C_t - bC_{t-1}\right)^{\eta\frac{1-\sigma}{\theta_V}}\left(1-N_t\right)^{(1-\eta)\frac{1-\sigma}{\theta_V}-2},
\end{aligned}$$

In steady state, we have:

$$\begin{aligned}
u_1 &= \eta\left(\left(1-b\right)C\right)^{\eta\left(\frac{1-\sigma}{\theta_V}\right)-1}\left(1-N\right)^{(1-\eta)\left(\frac{1-\sigma}{\theta_V}\right)}, \\
u_{11} &= \eta\left(\eta\left(\frac{1-\sigma}{\theta_V}\right)-1\right)\left(\left(1-b\right)C\right)^{\eta\left(\frac{1-\sigma}{\theta_V}\right)-2}\left(1-N\right)^{(1-\eta)\left(\frac{1-\sigma}{\theta_V}\right)}, \\
u_{12} &= -\eta\left((1-\eta)\left(\frac{1-\sigma}{\theta_V}\right)\right)\left(\left(1-b\right)C\right)^{\eta\left(\frac{1-\sigma}{\theta_V}\right)-1}\left(1-N\right)^{(1-\eta)\left(\frac{1-\sigma}{\theta_V}\right)-1}, \\
u_2 &= -\left(1-\eta\right)\left(\left(1-b\right)C\right)^{\eta\frac{1-\sigma}{\theta_V}}\left(1-N\right)^{(1-\eta)\frac{1-\sigma}{\theta_V}-1}, \\
u_{22} &= \left(1-\eta\right)\left(\left(1-\eta\right)\frac{1-\sigma}{\theta_V}-1\right)\left(\left(1-b\right)C\right)^{\eta\frac{1-\sigma}{\theta_V}}\left(1-N\right)^{(1-\eta)\frac{1-\sigma}{\theta_V}-2}.
\end{aligned}$$

Consequently, we can obtain:

$$\begin{aligned}
w &= -\frac{u_2}{u_1} = -\frac{-\left(1-\eta\right)\left(\left(1-b\right)C\right)^{\eta\frac{1-\sigma}{\theta_V}}\left(1-N\right)^{(1-\eta)\frac{1-\sigma}{\theta_V}-1}}{\eta\left(\left(1-b\right)C\right)^{\eta\left(\frac{1-\sigma}{\theta_V}\right)-1}\left(1-N\right)^{(1-\eta)\left(\frac{1-\sigma}{\theta_V}\right)}} = \frac{\left(1-\eta\right)\left(1-N\right)^{-1}}{\eta\left(\left(1-b\right)C\right)^{-1}} \\
&= \frac{\left(1-\eta\right)}{\eta}\frac{\left(1-b\right)C}{1-N}
\end{aligned}$$

and

$$\begin{aligned}\lambda &= \frac{wu_{11}+u_{12}}{u_{22}+wu_{12}} \\ &= \frac{\begin{array}{r}\left(\frac{(1-\eta)}{\eta}\frac{(1-b)C}{1-N}\right)\left(\eta\left(\eta\left(\frac{1-\sigma}{\theta_V}\right)-1\right)((1-b)C)^{\eta\left(\frac{1-\sigma}{\theta_V}\right)-2}(1-N)^{(1-\eta)\left(\frac{1-\sigma}{\theta_V}\right)}\right)+ \\ -\eta\left((1-\eta)\left(\frac{1-\sigma}{\theta_V}\right)\right)((1-b)C)^{\eta\left(\frac{1-\sigma}{\theta_V}\right)-1}(1-N)^{(1-\eta)\left(\frac{1-\sigma}{\theta_V}\right)-1}\end{array}}{\begin{array}{r}(1-\eta)\left((1-\eta)\frac{1-\sigma}{\theta_V}-1\right)((1-b)C)^{\eta\frac{1-\sigma}{\theta_V}}(1-N)^{(1-\eta)\frac{1-\sigma}{\theta_V}-2}+ \\ +\left(\frac{(1-\eta)}{\eta}\frac{(1-b)C}{1-N}\right)\left(-\eta\left((1-\eta)\left(\frac{1-\sigma}{\theta_V}\right)\right)((1-b)C)^{\eta\left(\frac{1-\sigma}{\theta_V}\right)-1}(1-N)^{(1-\eta)\left(\frac{1-\sigma}{\theta_V}\right)-1}\right)\end{array}}.\end{aligned}$$

Simplifying, we get:

$$\lambda = \frac{(1-N)}{(1-b)C}.$$

Derivation of the RRAs. We now have everything we need to derive the two expressions for the relative risk aversion. We put all the previously derived pieces in the expression:

$$RRA^{cl} = \frac{-u_{11}+\lambda u_{12}}{u_1}\cdot\frac{C+w(1-N)}{1+w\lambda}+\alpha\frac{(C+w(1-N))u_1}{u}$$

This implies:

$$\begin{aligned}RRA^{cl} = &\underbrace{\frac{\begin{array}{r}-\eta\left(\eta\left(\frac{1-\sigma}{\theta_V}\right)-1\right)((1-b)C)^{\eta\left(\frac{1-\sigma}{\theta_V}\right)-2}(1-N)^{(1-\eta)\left(\frac{1-\sigma}{\theta_V}\right)}+ \\ +\frac{(1-N)}{(1-b)C}\left(-\eta\left((1-\eta)\left(\frac{1-\sigma}{\theta_V}\right)\right)((1-b)C)^{\eta\left(\frac{1-\sigma}{\theta_V}\right)-1}(1-N)^{(1-\eta)\left(\frac{1-\sigma}{\theta_V}\right)-1}\right)\end{array}}{\eta((1-b)C)^{\eta\left(\frac{1-\sigma}{\theta_V}\right)-1}(1-N)^{(1-\eta)\left(\frac{1-\sigma}{\theta_V}\right)}}}_{PieceA}\cdot \\ &\underbrace{\frac{C+\left(\frac{(1-\eta)}{\eta}\frac{(1-b)C}{1-N}\right)(1-N)}{1+\frac{(1-\eta)}{\eta}\frac{(1-b)C}{1-N}\frac{(1-N)}{(1-b)C}}}_{PieceB} \\ &+\alpha\underbrace{\frac{\left(C+\left(\frac{(1-\eta)}{\eta}\frac{(1-b)C}{1-N}\right)(1-N)\right)\left(\eta((1-b)C)^{\eta\left(\frac{1-\sigma}{\theta_V}\right)-1}(1-N)^{(1-\eta)\left(\frac{1-\sigma}{\theta_V}\right)}\right)}{\frac{((1-b)C)^{\eta\frac{1-\sigma}{\theta_V}}(1-N)^{(1-\eta)\frac{1-\sigma}{\theta_V}}}{\frac{1-\sigma}{\theta_V}}}}_{PieceC}.\end{aligned}$$

Simplifying each piece, we get:

$$\begin{aligned} PieceA &= \left(1-\frac{1-\sigma}{\theta_V}\right)\frac{1}{(1-b)\,C}, \\ PieceB &= \frac{C\left(1+\frac{(1-\eta)}{\eta}(1-b)\right)}{1+\frac{(1-\eta)}{\eta}}, \\ PieceC &= \eta\left(\frac{1}{(1-b)}+\frac{(1-\eta)}{\eta}\right)\frac{1-\sigma}{\theta_V}. \end{aligned}$$

So, putting all together, we have:

$$R^{cl} = \underbrace{\left(1-\frac{1-\sigma}{\theta_V}\right)\frac{1}{(1-b)\,C}\cdot\frac{C\left(1+\frac{(1-\eta)}{\eta}(1-b)\right)}{1+\frac{(1-\eta)}{\eta}}}_{pieceA\cdot pieceB} + \alpha\cdot\underbrace{\eta\left(\frac{1}{(1-b)}+\frac{(1-\eta)}{\eta}\right)\frac{1-\sigma}{\theta_V}}_{pieceC}$$

which, once we replace the definition of θ_V with its expression, becomes:

$$RRA^{cl} = \frac{1}{\psi}\cdot\frac{\left(1+\frac{(1-\eta)}{\eta}(1-b)\right)}{(1-b)\left(1+\frac{(1-\eta)}{\eta}\right)} + \alpha\left(\frac{\eta}{(1-b)}+1-\eta\right)\left(1-\frac{1}{\psi}\right)$$

Replacing $\alpha = \left(1-\frac{1-\sigma}{1-\frac{1}{\psi}}\right)$, and simplifying:

$$RRA^{cl} = \frac{1}{\psi}\cdot\frac{\left(1+\frac{(1-\eta)}{\eta}(1-b)\right)}{(1-b)\left(1+\frac{(1-\eta)}{\eta}\right)} + \left(\sigma-\frac{1}{\psi}\right)\left(\frac{\eta}{(1-b)}+1-\eta\right),$$

which delivers $RRA^{cl}=\sigma$ when the degree of external habits $b=0$.

Finally:

$$\begin{aligned} RRA^{cl} &= \left(1+\frac{w}{C}(1-N)\right)RRA^{c} \\ &= \left(\frac{\eta}{\eta+(1-\eta)(1-b)}\right)RRA^{cl} \end{aligned}$$

This implies:

$$RRA^{c} = \left(\frac{\eta}{\eta+(1-\eta)(1-b)}\right)\cdot\left(\frac{1}{\psi}\cdot\frac{\left(1+\frac{(1-\eta)}{\eta}(1-b)\right)}{(1-b)\left(1+\frac{(1-\eta)}{\eta}\right)} + \left(\sigma-\frac{1}{\psi}\right)\left(\frac{\eta}{(1-b)}+1-\eta\right)\right).$$

This is exactly the expression used in the paper to compute the RRA.

E: Mimimum distance estimation strategy

The state-dependent Bayesian minimum distance estimator works as follows. Denote by $\widehat{\boldsymbol{\psi}^i}$ the vector in which we stack the (I)VAR estimated (generalized) impulse responses over a 20-quarter horizon to an uncertainty shock for each regime $i = 1, 2$ (i.e., the responses displayed in Figure 2).[9] When the number of observations per regime n^i is large, standard asymptotic theory suggests that

$$\widehat{\boldsymbol{\psi}^i} \overset{a}{\sim} N(\boldsymbol{\psi}\left(\boldsymbol{\zeta}_0^i\right), \mathbf{V}^i(\boldsymbol{\zeta}_0^i, n^i)), \text{ for } i = 1, 2 \tag{1}$$

where $\boldsymbol{\zeta}_0^i$ denotes the true vector of structural parameters that we estimate ($i = 1, 2$) and $\boldsymbol{\psi}\left(\boldsymbol{\zeta}^i\right)$ denotes the model-implied mapping from a vector of parameters to the analog impulse responses in $\widehat{\boldsymbol{\psi}^i}$.

As explained earlier, the IVAR GIRFs $\widehat{\boldsymbol{\psi}^i}$ for the great recession are computed by iterating forward the system starting from the initial condition $t-1 = 2008Q3$, whereas the IRFs for the linear VAR are the standard IRFs which refer to the unconditional mean of the variables. Similarly, we compute the DSGE model-related responses for each given set of parameter values $\boldsymbol{\psi}\left(\boldsymbol{\zeta}^i\right)$ by iterating forward the approximated solution of the DSGE model starting from the (state-specific in our case) stochastic steady state.[10] Both DSGE-based and VAR-based impulse responses are interpreted as percent deviations of variables induced by an uncertainty shock, with the exception - in our case - of the interest rate response which is measured in percentage points as implied by the VAR specification.

To compute the posterior density for $\boldsymbol{\zeta}^i$ given $\widehat{\boldsymbol{\psi}^i}$ using Bayes' rule, we first need to compute the likelihood of $\widehat{\boldsymbol{\psi}^i}$ conditional on $\boldsymbol{\zeta}^i$. Given (1), the approximate likelihood

[9] For a paper proposing information criteria to select the responses that produce consistent estimates of the true but unknown structural parameters and those that are most informative about DSGE model parameters, see Hall, Inoue, Nason, and Rossi (2012).

[10] Following Basu and Bundick (2017), we set the value of the exogenous processes to zero and iterate forward until the model converges to its stochastic steady state. Then, we hit the model with an uncertainty shock of the same size as in the IVAR (i.e., a 4.4 standard deviation shock) and compute impulse responses as the percent deviation between the stochastic path followed by the endogenous variables and their stochastic steady state. Given that no future shocks are considered, this way of computing GIRFs does not line up with Koop, Pesaran and Potter's (1996) algorithm. We do so to avoid simulating the model several times and then integrate across all simulations, a procedure which would be very time consuming, above all when combined with the MCMC algorithm we adopt for our Bayesian estimation. Basu and Bundick (2017) show that the differences between these two ways of computing GIRFs are negligible with a framework like theirs. We also verified that our IVAR GIRFs remained unchanged when future shocks are not taken into account, something which augments the comparability between IVAR and DSGE GIRFs. Analytical expressions for GIRFs produced with nonlinear models are available in Andreasen, Fernández-Villaverde, and Rubio-Ramírez (2018).

of $\widehat{\boldsymbol{\psi}^i}$ as a function of $\boldsymbol{\zeta}^i$ reads as follows:

$$f(\widehat{\boldsymbol{\psi}^i}|\boldsymbol{\zeta}^i) = \left(\frac{1}{2\pi}\right)^{\frac{N^i}{2}} \left|\mathbf{V}^i(\boldsymbol{\zeta}_0^i, n^i)\right|^{-\frac{1}{2}} \times \exp\left[-\frac{1}{2}\left(\widehat{\boldsymbol{\psi}^i} - \boldsymbol{\psi}\left(\boldsymbol{\zeta}^i\right)\right)' \mathbf{V}^i(\boldsymbol{\zeta}_0^i, n^i)^{-1}\left(\widehat{\boldsymbol{\psi}^i} - \boldsymbol{\psi}\left(\boldsymbol{\zeta}^i\right)\right)\right] \tag{2}$$

where N^i denotes the number of elements in $\widehat{\boldsymbol{\psi}^i}$ and $\mathbf{V}^i(\boldsymbol{\zeta}_0^i, n^i)$ is treated as a fixed value.[11] We use a consistent estimator of $\mathbf{V}^i$. Because of small sample-related considerations, such estimator features only diagonal elements (see Christiano, Trabandt, and Walentin (2011) and Guerron-Quintana, Inoue, and Kilian (2017)).[12] In our case, $\mathbf{V}^i$ is a regime-dependent diagonal matrix with the variances of the $\widehat{\boldsymbol{\psi}^i}$ along the main diagonal.[13] This choice is widely adopted in the literature and allows one to put more weight in replicating VAR-based responses with relatively smaller confidence bands. Treating eq. (2) as the likelihood function of $\widehat{\boldsymbol{\psi}^i}$, it follows that the Bayesian posterior of $\boldsymbol{\zeta}^i$ conditional on $\widehat{\boldsymbol{\psi}^i}$ and $\mathbf{V}^i$ is:

$$f(\boldsymbol{\zeta}^i|\widehat{\boldsymbol{\psi}^i}) = \frac{f(\widehat{\boldsymbol{\psi}^i}|\boldsymbol{\zeta}^i)p(\boldsymbol{\zeta}^i)}{f(\widehat{\boldsymbol{\psi}^i})}, \tag{3}$$

where $p(\boldsymbol{\zeta}^i)$ denotes the priors on $\boldsymbol{\zeta}^i$ and $f(\widehat{\boldsymbol{\psi}^i})$ is the marginal density of $\widehat{\boldsymbol{\psi}^i}$. As in Christiano, Trabandt, and Walentin (2011), the mode of the posterior distribution of $\boldsymbol{\zeta}^i$ is computed by maximizing the value of the numerator in 3 via the csminwel

[11] As pointed out by Christiano, Eichenbaum, and Trabandt (2016) and Bundick and Smith (2019), there are four reasons why this is only an approximate likelihood. First, standard asymptotic theory implies that, if the DSGE model is the correct data generating process with the true parameters $\boldsymbol{\zeta}_0^i$, $\widehat{\boldsymbol{\psi}^i}$ converges only asymptotically to $N(\boldsymbol{\psi}(\boldsymbol{\zeta}_0^i), \mathbf{V}^i)$ as the sample size grows arbitrarily large. Second, our proxy for $\mathbf{V}^i$ is guaranteed to be correct only as the sample size grows arbitrarily large. Third, $\boldsymbol{\psi}^i$ is approximated with a nonlinear model approximated at a third order, i.e., not with the true, global nonlinear model. Fourth, differently from the linear model case, the IRFs are not a full summary of nonlinear frameworks.

[12] Guerron-Quintana, Inoue, and Kilian (2017) study the asymptotic theory for VAR-based impulse response matching estimators of the structural parameters of linearized DSGE models when the number of impulse responses exceeds the number of linear VAR model parameters. The number of impulse responses in our analysis (140) is lower than the number of estimated coefficients of the VAR (251, constants excluded). We are aware of no contributions studying the asymptotic theory for this estimator when nonlinear frameworks are employed.

[13] Denoting by $\hat{\mathbf{W}}^i$ the bootstrapped variance-covariance matrix of VAR-based impulse responses $\widehat{\boldsymbol{\psi}}^i$ for regime i, i.e., $\frac{1}{M}\sum_{j=1}^{M}(\boldsymbol{\psi}_j^i - \bar{\boldsymbol{\psi}}^i)(\boldsymbol{\psi}_j^i - \bar{\boldsymbol{\psi}}^i)'$ (where $\boldsymbol{\psi}_j^i$ denotes the realization of $\widehat{\boldsymbol{\psi}}^i$ in the j^{th} (out of $M = 1,000$) bootstrap replication and $\bar{\boldsymbol{\psi}}^i$ denotes the mean of $\boldsymbol{\psi}_j^i$), $\mathbf{V}^i$ is based on the diagonal of this matrix. Notice that $\mathbf{V}^i$ contains the same variances that will be used to plot the confidence intervals for the I-VAR responses in next Section. This is the same approach used in Altig, Christiano, Eichenbaum, and Lindé (2011).

algorithm proposed by Chris Sims.[14] The posterior densities are estimated via Laplace approximation.

F: Model calibration

We calibrate some of the parameters of the model as in Basu and Bundick (2018), the reason being that we use a slightly modified version of their model (to which we add habits in consumption) for our analysis. Table A2 collects all the calibrated parameters. We do not estimate these parameters for several reasons. We follow a long tradition in macroeconomics and calibrate the capital's share in production α, the household discount factor β and the steady state depreciation rate δ to values that are standard in the literature. The first-order utilization parameter δ_1 and the consumption weight in the period utility function η cannot be estimated, because the first is determined endogenously by a steady state relationship (involving δ and β) and the second is fixed in order to imply a Frisch elasticity equal to 2. The steady state inflation rate Π cannot be estimated by a impulse response functions matching procedure that focuses on out-of-steady state dynamics, i.e., deviations from the (stochastic) steady state. The firm leverage parameter ν does not influence impulse responses in the absence of financial frictions and hence is not identified. As regards the parameters of the stochastic shock processes, we calibrate the volatility of the second moment preference shock σ_{σ^a} to the same value as calibrated in Basu and Bundick (2018) to match empirical moments. The parameters governing the processes of the preference and technological shocks, i.e. ρ^a, σ^a, ρ^Z and σ^Z are calibrated by borrowing values from Basu and Bundick (2018). In spite of our focus on the effects of the uncertainty shocks, we calibrate also these parameters because these stochastic processes can in principle influence (even on-impact) the response of the model-consistent VXO to an uncertainty shock. We also do not estimate the second-order utilization parameter δ_2, the elasticity of substitution between intermediate goods θ_μ, and the IES ψ to not further increase the computational burden of the estimation procedure.

[14] The use of a direct inference approach to estimate the DSGE model is justified by the Monte Carlo analysis reported in Appendix C. There we show that the narrative sign restriction identification approach we use in our VAR analysis recovers the true impulse responses produced by the DSGE framework.

G: Counterfactuals to identify relevant parameter instabilities

We conduct counterfactual exercises to identify the relevant parameters affecting the impulse responses of the variables of interest to an uncertainty shock. We check the impact of each parameter on the impulse responses produced by the DSGE model as follows. Conditional on the set of estimates based on the linear VAR case, we replace the value of each parameter with the corresponding estimated value in the great recession. The design of these exercises implies that if we replaced all estimated parameters contemporaneously, by construction we would replicate the impulse responses produced by the DSGE in the great recession. Figures A8 and A9 display the outcome of our analysis. The three key parameters for the change in the impulse responses when moving from normal times to the 2007-09 extreme event are the parameter influencing the degree of risk aversion, that regulating the adjustment costs of investment, and the Taylor rule parameter related to output growth. Table A3 reports the set of estimated parameters (already presented in the text of the paper, and replicated here for the sake of completeness).

H: Role of initial conditions in the nonlinear DSGE model

This Section investigates whether the initial conditions in the nonlinear DSGE model we employ play a role for the dynamics of the system after an uncertainty shock. Andreasen, Fernández-Villaverde, and Rubio-Ramírez (2018) show that the initial values of the states are potentially very important for the effects of the macroeconomic shocks they study. The computation of the GIRFs in our paper follows Basu and Bundick (2017) and do not take into account the role of initial conditions. Hence, this possible omitted factor could be behind the evidence of countercyclical risk aversion we find.[15] It is therefore important to provide a check on the relevance of initial conditions in the model we work with.

Cacciatore and Ravenna (2018) prove that pruning the third-order approximation completely eliminates state dependence in the propagation of uncertainty shocks. Hence, to check the relevance of initial conditions we switch to the unpruned third-order approximation of our model. In particular, a Monte Carlo exercise with artificial data simulated with the Basu and Bundick (2017) framework is conducted. The exercise is

[15] As explained in the main text, we compute responses in the model starting from the regime-specific stochastic steady state implied by the estimated set of parameters. As in Basu and Bundick (2017,2018), we adopt the pruned third-order approximation proposed in Andreasen, Fernández-Villaverde, and Rubio-Ramírez (2017).

conducted similarly to Section C of this Appendix, but with two differences. First, here the unpruned approximated solution is used to simulate the model. Second, on top of the linear VAR, also an IVAR model similar to the one adopted in the baseline analysis is estimated on the simulated data.

Figure A10 compares the linear VAR response and the IVAR response for a (model-consistent) very deep contraction.[16] The identified set of the linear VAR and IVAR responses lie literally on top of each other. Hence results show that the initial conditions in the DSGE model do not materially influence the computed GIRFs to an uncertainty shock, i.e., no endogenous state-dependence is generated in the DSGE model with the use of the standard workhorse solution methods.[17]

[16] We compute the IVAR response for the initial condition corresponding to the deepest contraction in the simulated sample.

[17] We were prevented to conduct a similar exercise using a forth order approximation due to large approximation errors that caused severely distorted GIRFs. In a companion paper, Andreasen, Caggiano, Castelnuovo, and Pellegrino (2020), we use an approximation around the risky steady state, rather than around the deterministic steady state, so that to both allow initial conditions to play a role for the propagation of uncertainty shocks and accurately solve nonlinear DSGE models.

References

Altig, D., L. J. Christiano, M. Eichenbaum, and J. Lindé (2011): "Firm-Specific Capital, Nominal Rigidities and the Business Cycle," *Review of Economic Dynamics*, 14(2), 225–247.

Andreasen, M., G. Caggiano, E. Castelnuovo, and G. Pellegrino (2020): "Uncertainty-Driven Comovements in Booms and Busts: A Structural Intepretation," Aarhus University, Monash University, and University of Melbourne, in progress.

Andreasen, M. M., J. Fernández-Villaverde, and J. F. Rubio-Ramírez (2018): "The Pruned State-Space System for Non-Linear DSGE Models: Theory and Empirical Applications," *Review of Economic Studies*, 85(1), 1–49.

Basu, S., and B. Bundick (2017): "Uncertainty Shocks in a Model of Effective Demand," *Econometrica*, 85(3), 937–958.

Basu, S., and B. Bundick (2018): "Uncertainty Shocks in a Model of Effective Demand: Reply," *Econometrica*, 86(4), 1527–1531.

Bloom, N. (2009): "The Impact of Uncertainty Shocks," *Econometrica*, 77(3), 623–685.

Bundick, B., and A. L. Smith (2019): "The Dynamic Effects of Forward Guidance Shocks," *Review of Economics and Statistics*, forthcoming.

Cacciatore, M., and F. Ravenna (2018): "Uncertainty, Wages, and the Business Cycle," HEC Montreal, mimeo.

Christiano, L., M. Eichenbaum, and M. Trabandt (2016): "Unemployment and Business Cycles," *Econometrica*, 84(4), 1523–1569.

Christiano, L., M. Trabandt, and K. Walentin (2011): "DSGE Models for Monetary Policy Analysis," in: B. M. Friedman and M. Woodford (Eds.): Handbook of Monetary Economics, Volume 3a, 285–367.

Christiano, L. J., M. Eichenbaum, and C. Evans (1999): "Monetary Policy Shocks: What Have We Learned and to What End?," In: J.B. Taylor and M. Woodford (eds.): Handbook of Macroeconomics, Elsevier Science, 65–148.

Fry, R., and A. Pagan (2011): "Sign Restrictions in Structural Vector Autoregressions: A Critical Review," *Journal of Economic Literature*, 49(4), 938–960.

Gilchrist, S., and E. Zakrajšek (2012): "Credit Spreads and Business Cycle Fluctuations," *American Economic Review*, 102(4), 1692–1720.

Guerron-Quintana, P., A. Inoue, and L. Kilian (2017): "Impulse Response Matching Estimators for DSGE Models," *Journal of Econometrics*, 196, 144–155.

Hall, A., A. Inoue, J. Nason, and B. Rossi (2012): "Information Criteria for Impulse Response Function Matching Estimation of DSGE Models," *Journal of Econometrics*, 170(2), 499–518.

Kilian, L., and R. Vigfusson (2011): "Are the Responses of the U.S. Economy Asymmetric in Energy Price Increases and Decreases?," *Quantitative Economics*, 2, 419–453.

Koop, G., M. Pesaran, and S. Potter (1996): "Impulse response analysis in nonlinear multivariate models," *Journal of Econometrics*, 74(1), 119–147.

Ludvigson, S. C., S. Ma, and S. Ng (2019): "Uncertainty and Business Cycles: Exogenous Impulse or Endogenous Response?," *American Economic Journal: Macroeconomics*, forthcoming.

Rudebusch, G. D., and E. T. Swanson (2012): "The Bond Premium in a DSGE Model with Long-Run Real and Nominal Risks," *American Economic Journal: Macroeconomics*, 4(1), 105–143.

Stock, J. H., and M. W. Watson (2012): "Disentangling the Channels of the 2007-2009 Recession," *Brookings Papers on Economic Activity*, Spring, 81–135.

Swanson, E. T. (2012): "Risk Aversion and the Labor Margin in Dynamic Equilibium Models," *American Economic Review*, 102, 1663–1691.

——— (2018): "Risk Aversion, Risk Premia, and the Labor Margin with Generalized Recursive Preferences," *Review of Economic Dynamics*, 28, 290–321.

	Output	Consumpt.	Investment	Hours
Baseline IVAR and VAR				
Peak response: Linear	-1.54%	-1.03%	-3.34%	-1.90%
Peak response: Great Recession	-2.32%	-1.36%	-8.32%	-3.75%
Ratio GR/Linear	1.50	1.32	2.49	1.97
IVAR and VAR with financial spread				
Peak response: Linear	-1.58%	-0.78%	-3.70%	-1.63%
Peak response: Great Recession	-2.44%	-1.10%	-8.11%	-3.33%
Ratio GR/Linear	1.54	1.41	2.19	2.04

Table A1: **Peak responses.** Peak responses to a one standard deviation uncertainty shock estimated with linear VAR and nonlinear IVAR for the great recession

Par.	Description	Value
σ_{σ^a}	volatility of the uncertainty shock	0.004
ρ^a	persistence of the preference shock	0.98
σ^a	volatility of the preference shock	0.005
ρ^Z	persistence of the technology shock	0.35
σ^Z	volatility of the technology shock	0.019
α	capital's share in production	0.333
β	household discount factor	0.994
δ	steady state depreciation rate	0.025
δ_1	first-order utilization parameter	$1/\beta - 1 + \delta$
Π	steady state inflation rate	1.005
ν	firm leverage parameter	0.9
δ_2	second-order utilization parameter	0.0003
θ_μ	elasticity of subst. between intermediate goods	6.0
ψ	intertemporal elasticity of substitution	0.5

Table A2: **DSGE model: Calibrated parameters. Calibration borrowed from Basu and Bundick (2018).**

		Priors	Posteriors	
			Linear VAR	Great Recession
Parameter	Interpretation	D(mean, std)	Mode, std	Mode, std
ρ_{σ^a}	Unc.shock,pers.	B(0.77, 0.10)	**0.64,** 0.03	**0.65,** 0.03
b	Habit formation parameter	B(0.75, 0.15)	**0.64,** 0.06	**0.66,** 0.04
ϕ_K	Investment adjustment costs	G(3.92, 2)	**2.29,** 0.50	**3.21,** 0.60
ϕ_P	Price adjustment costs	G(240, 40)	**236.78,** 32.26	**282.10,** 33.54
ρ_π	Taylor rule parameter, inflation	IG(1.5, 0.25)	**1.05,** 0.01	**1.05,** 0.01
ρ_y	Taylor rule parameter, output growth	G(0.2, 0.15)	**0.20,** 0.04	**0.28,** 0.05
σ	Risk aversion (fixed labor supply, no habits)	G(100, 60)	**385.90,** 50.45	**533.04,** 59.16
RRA	Risk aversion (endogenous labor supply, habits)		**104.85**	**144.96**

Table A3: **DSGE model: Average evidence vs. Great recession.** Values estimated conditional on both the linear VAR impulse responses and on the IVAR impulse responses in 2008Q4. Standard deviations estimated conditional on a Laplace approximation of the posterior density. Risk aversion in the model (RRA) computed by considering endogenous labor supply and habits as in Swanson (2018).

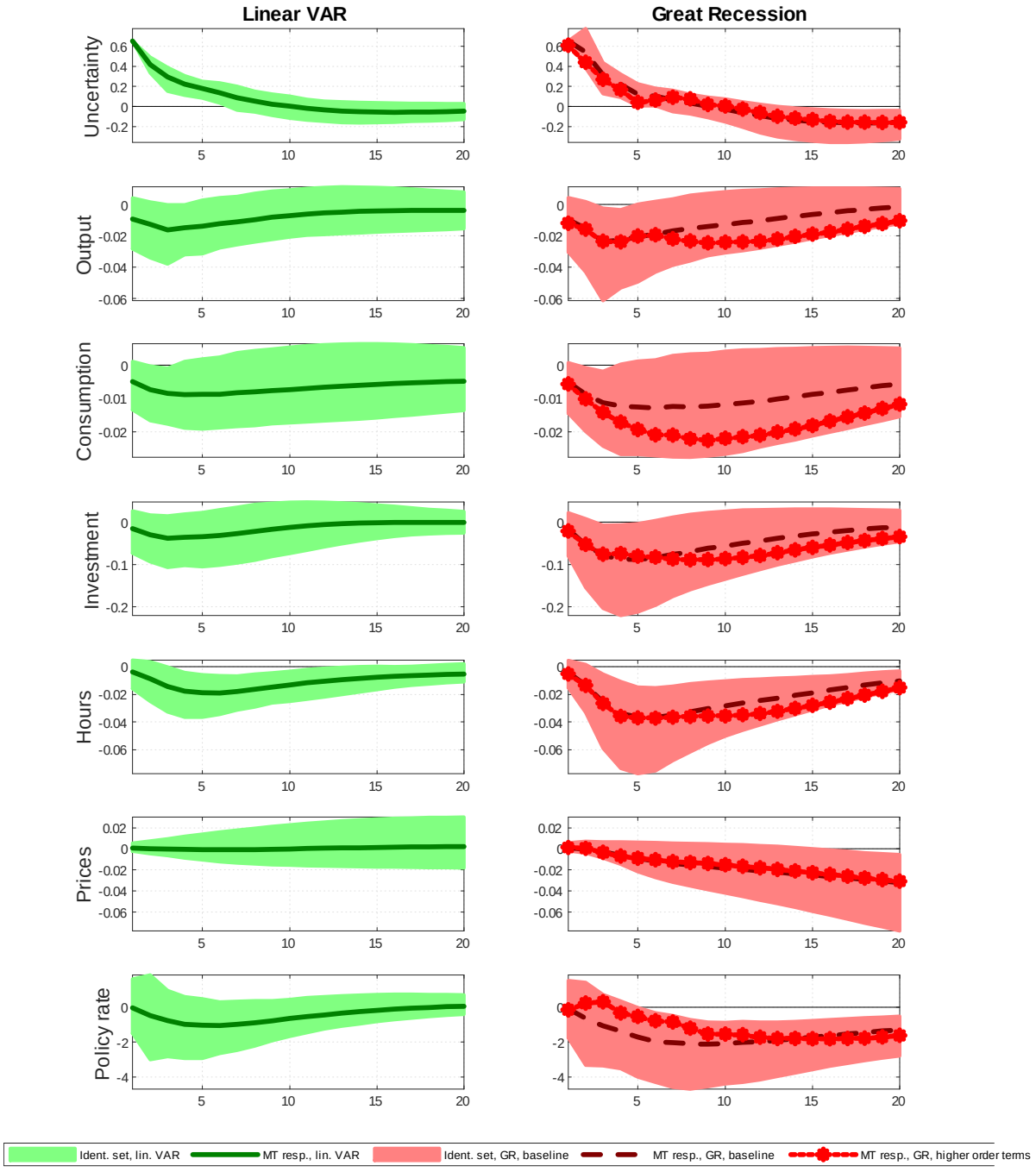

Figure A1: **IVAR impulse responses: Role of higher order terms.** Areas in the first and second columns: Identified set for impulse responses produced with the baseline, parsimonious IVAR. Solid green and dashed dark red lines in the first and second columns: Impulse responses produced with the baseline, parsimonious IVAR. Lines with red stars (second columns): Impulse responses produced with the expanded IVAR featuring extra-interaction terms.

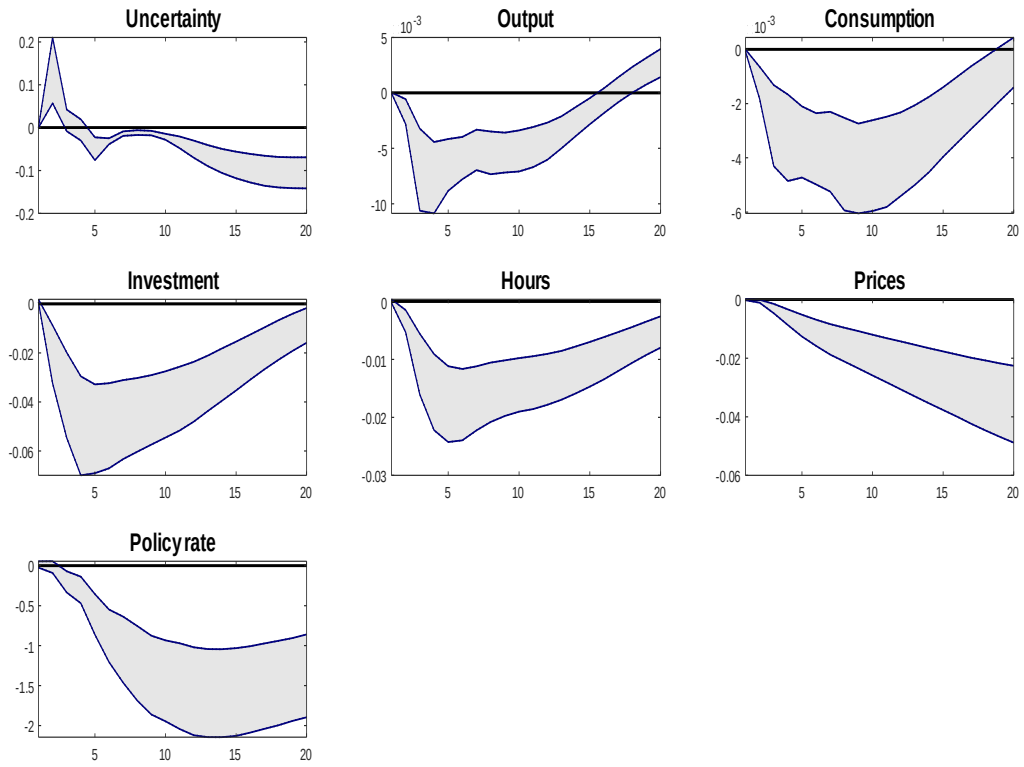

Figure A2: **Test for the difference of responses that focuses on model uncertainty.** The test takes into account the correlation between the responses. 90% confidence bands in gray.

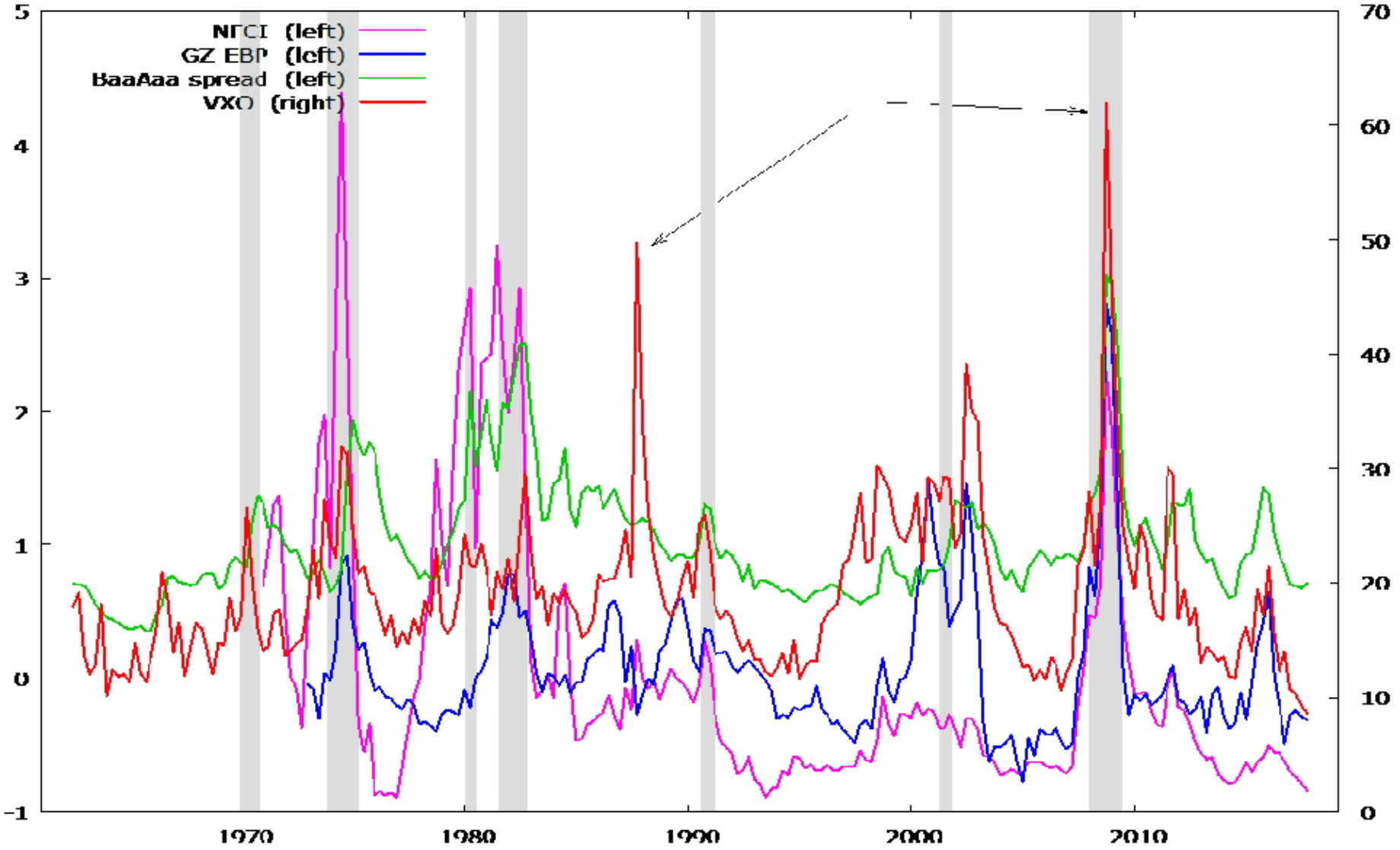

Figure A3: **VXO against common financial stress indicators.** Arrows indicate the 1987Q4 and 2008Q4 spikes in the VXO. Indicators of financial stress (related to first-moment financial shocks): NFCI = National Financial Conditions Index produced by the Federal Reserve Bank of Chicago; GZ EBP = Excess Bond Premium by Gilchrist and Zakrajï£¡ek (2012); BaaAaa spread = spread computed by subtracting the AAA yield from the BAA one.

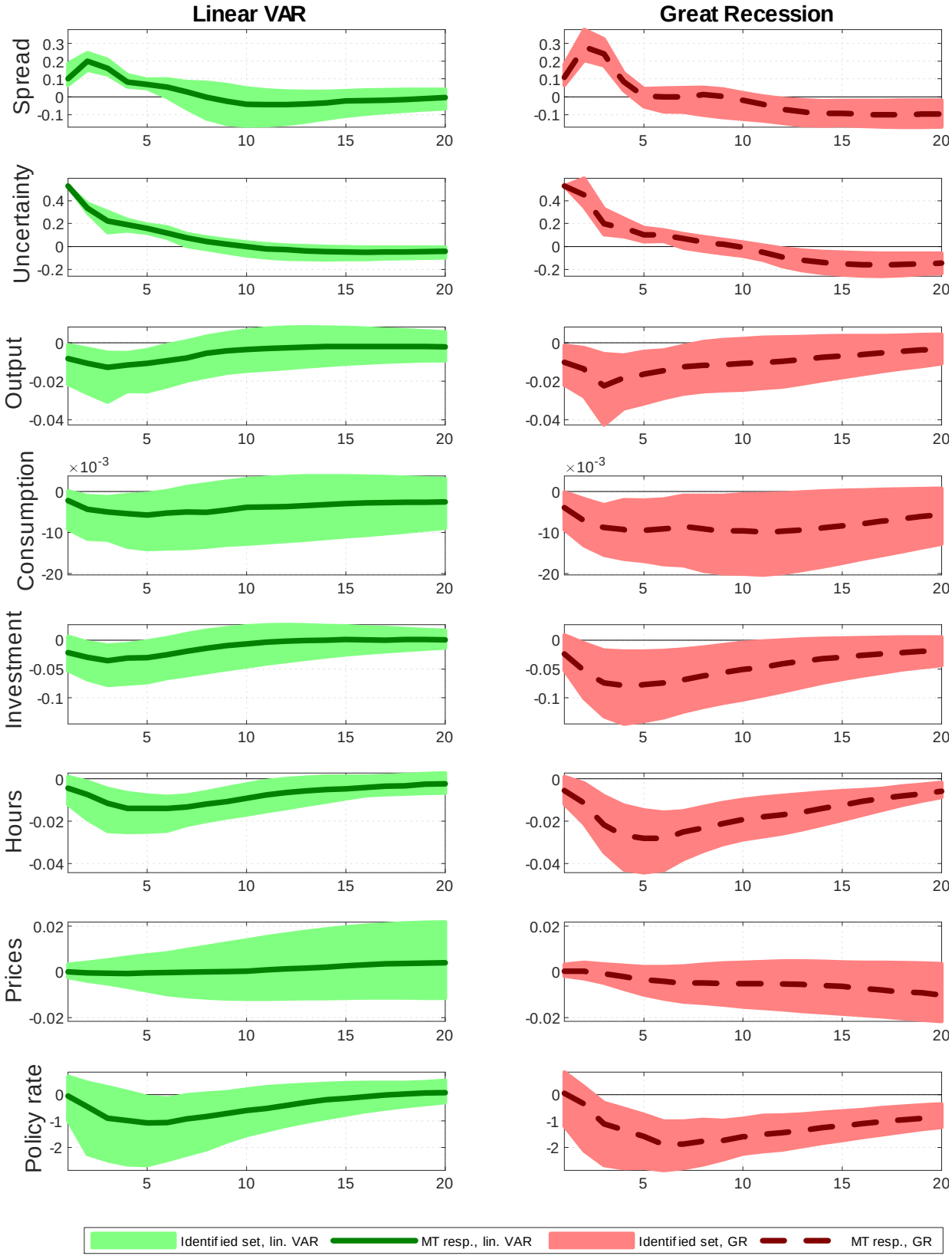

Figure A4: **Credit Spread. Impulse responses: linear vs. great recession.** Impulse responses to a one-standard deviation uncertainty shock. The solid green (red) areas report the identified set of responses for the linear (nonlinear) VAR models. The solid (dashed) lines report the median target impulse response for the linear (nonlinear) VAR. The number of retained draws, out a total of one million draws, is 2168 for IVAR and 2116 for linear VAR.

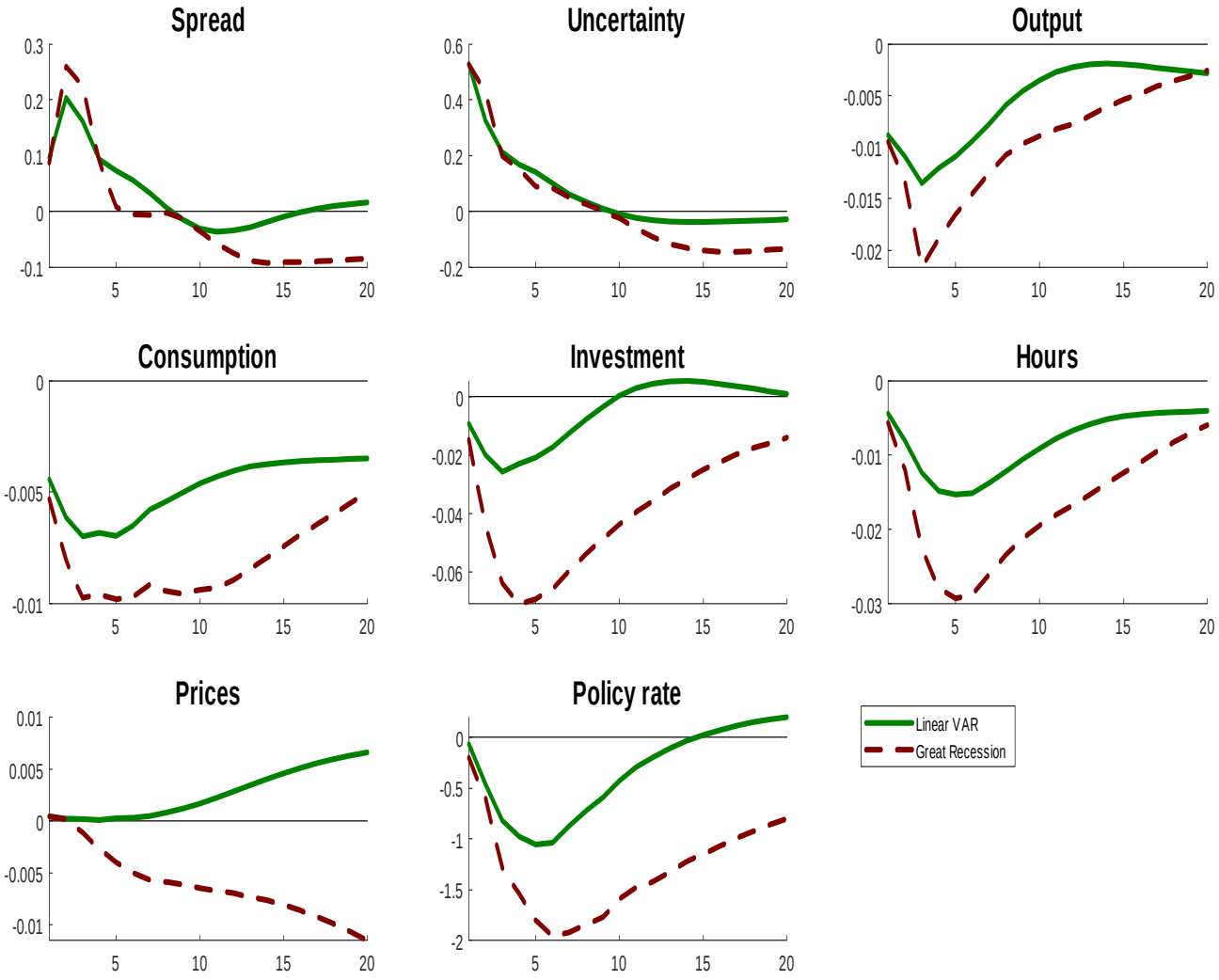

Figure A5: **Credit spread. Impulse responses: Fry and Pagan (2011) median target IRFs.** The solid green line reports the median target (MT) impulse response for the linear VAR. The dashed red line is the MT impulse response obtained from the IVAR for the great recession.

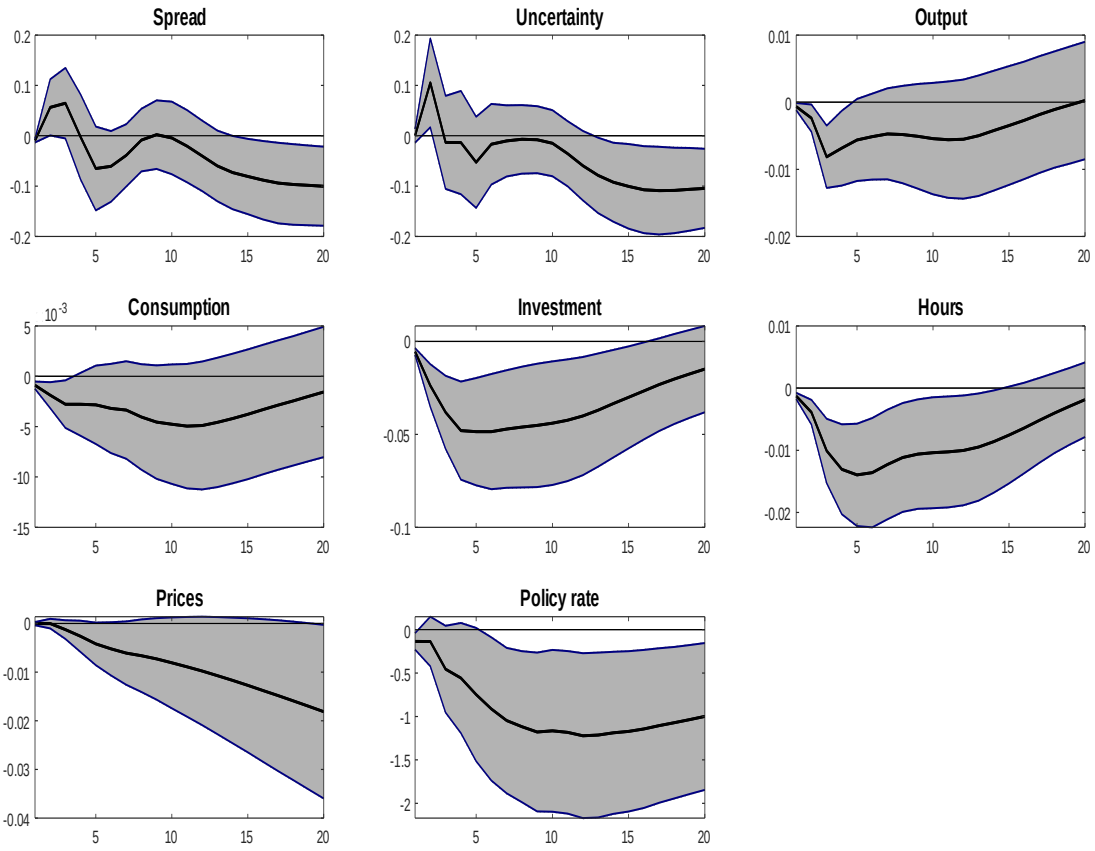

Figure A6: **Credit spread. Bootstrapped test for the difference of median target responses.** 90% confidence bands in gray.

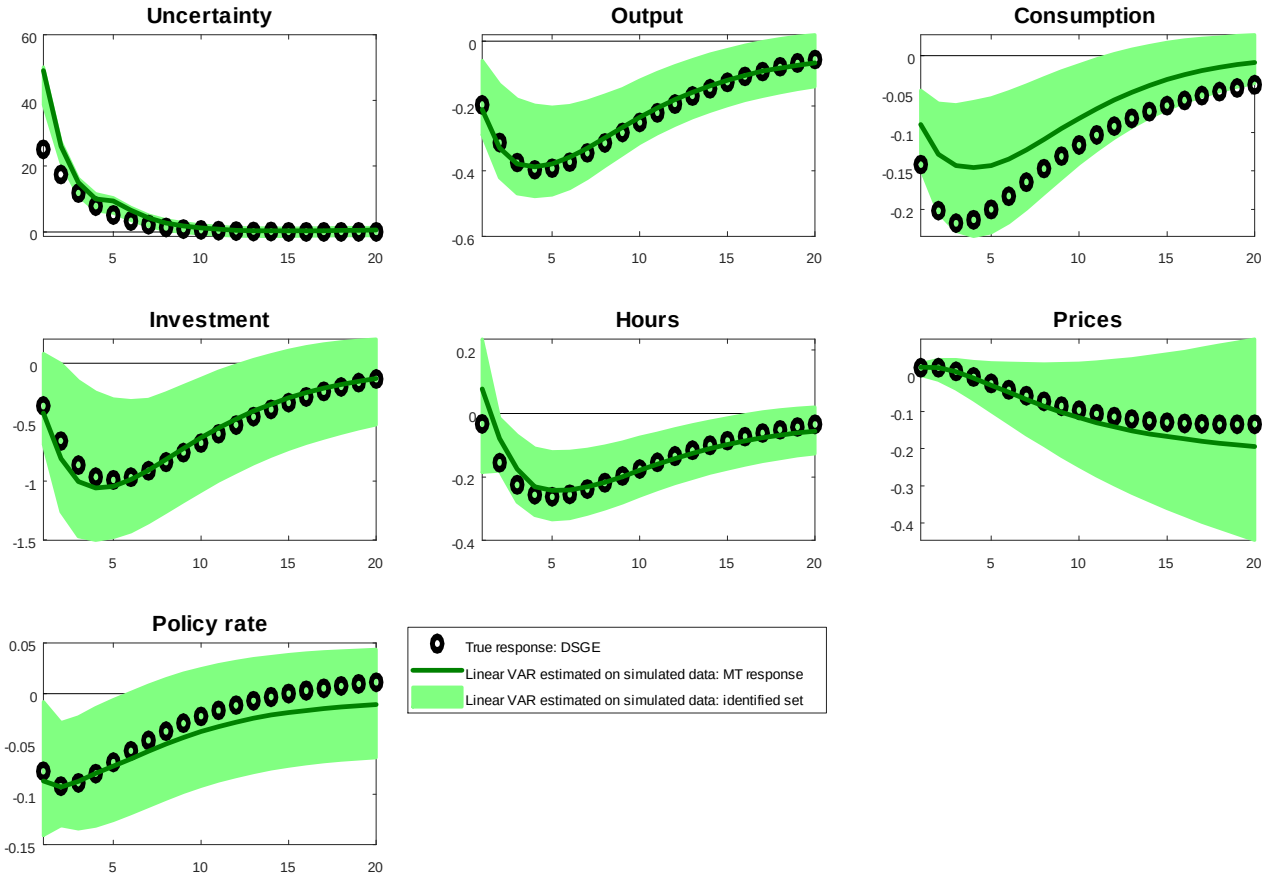

Figure A7: **Monte Carlo simulation: DSGE model vs. VAR responses to an uncertainty shock**. Calibration of the DSGE model with the estimates we obtained with the facts established by the linear VAR. Size of the simulated sample: 2,500 observations (100 of which are used as burnin). Consistently with our baseline analysis, uncertainty shocks are identified by exploiting the dates corresponding to the biggest spikes of the HP-filtered model-implied VXO, as explained in the text.

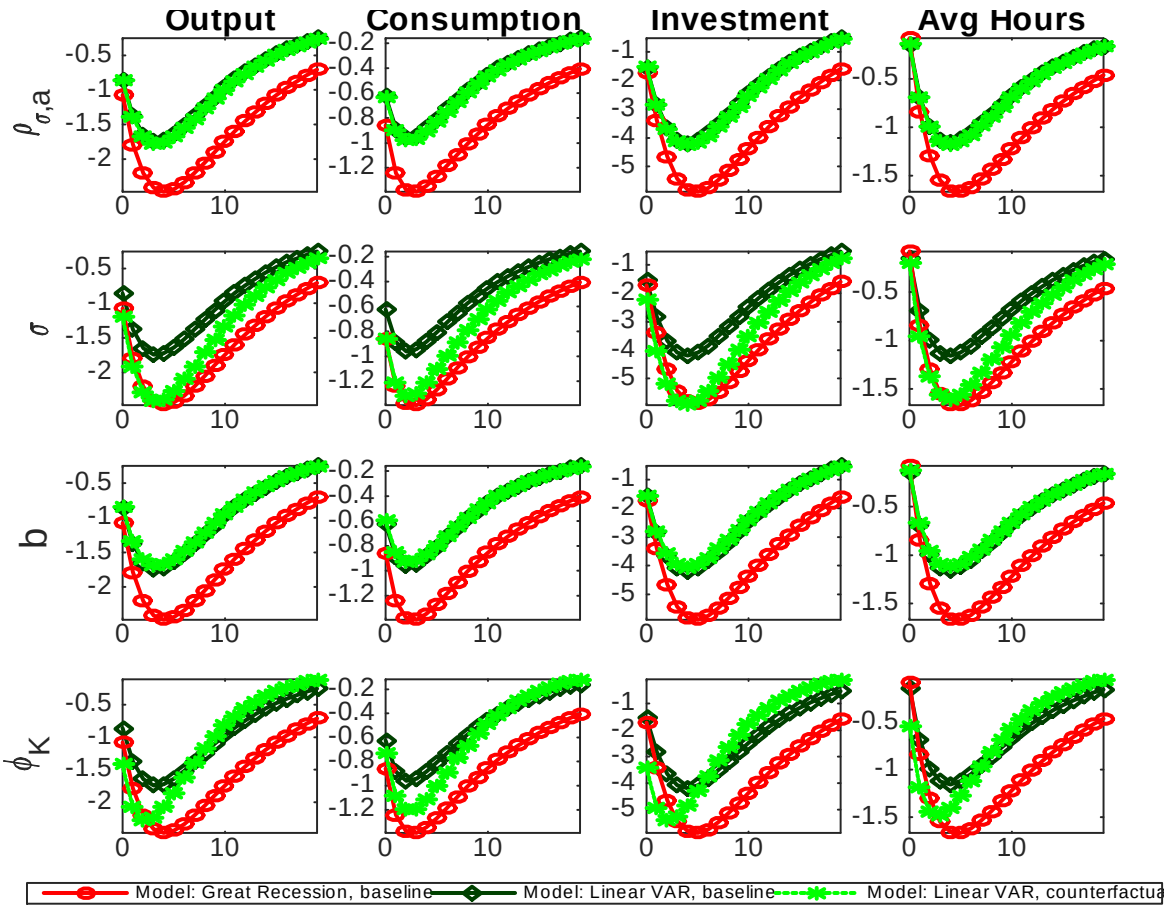

Figure A8: **Role of structural parameters for the great recession-contingent IRFs produced by the DSGE model: First set of parameters.** Red line with circles: Model estimated with great recession impulse responses. Black line with diamonds: Model estimated with linear VAR impulse responses. Green line with stars: Model calibrated with normal times estimates but one parameter, which is the one indicated with the label on the y-axis, and which is calibrated with its great recession estimate. Exercise conducted by starting from the estimates based on the linear VAR case and replacing the value of each structural parameter (one at a time) with the corresponding estimated value conditional on the great recession impulse responses.

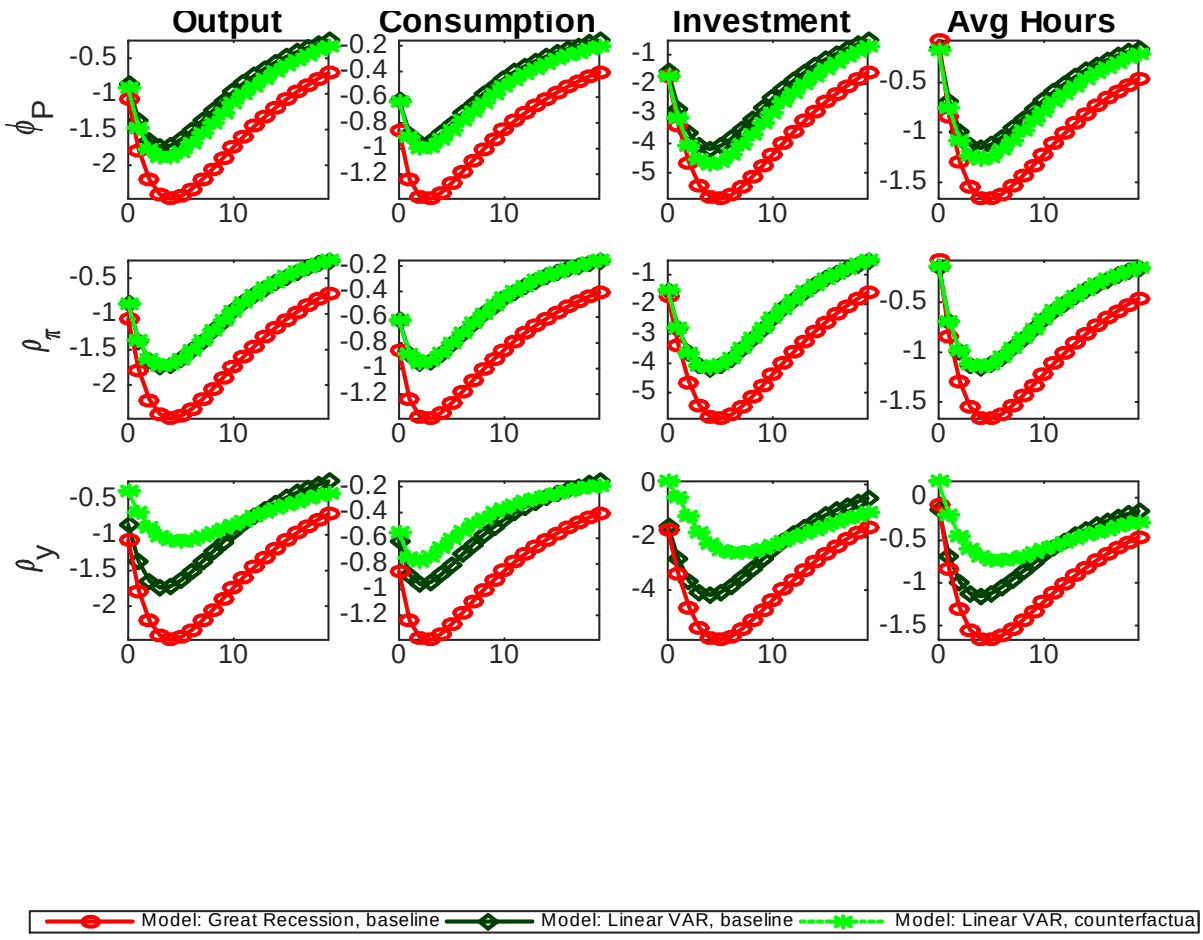

Figure A9: **Role of structural parameters for the great recession-contingent IRFs produced by the DSGE model: Second set of parameters.** Red line with circles: Model estimated with great recession impulse responses. Black line with diamonds: Model estimated with linear VAR impulse responses. Green line with stars: Model calibrated with normal times estimates but one parameter, which is the one indicated with the label on the y-axis, and which is calibrated with its great recession estimate. Exercise conducted by starting from the estimates based on the linear VAR case and replacing the value of each structural parameter (one at a time) with the corresponding estimated value conditional on the great recession impulse responses.

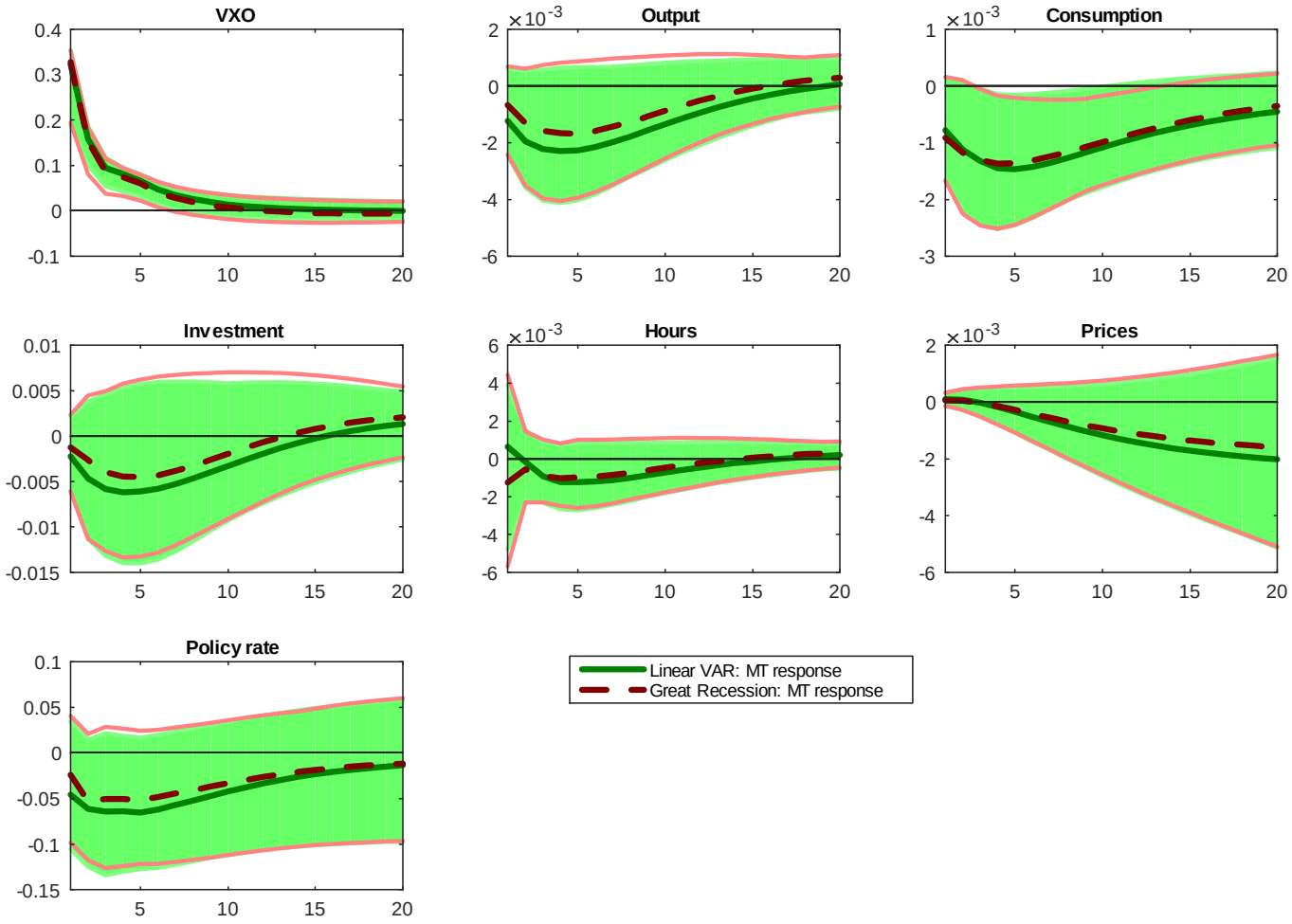

Figure A10: **Monte Carlo simulation: DSGE model vs. IVAR responses to an uncertainty shock for a model-implied very deep contraction**. Calibration of the DSGE model with the estimates we obtained with the facts established by the linear VAR. Size of the simulated sample: 2,500 observations (100 of which are used as burnin). Uncertainty shocks are identified by exploiting the information coming from the biggest spikes of the HP-filtered model-implied VXO, as explained in the text. Green areas and white area delimited by solid red lines: identified set for the linear VAR and IVAR response, respectively.